NTNU

Norwegian University of
Science and Technology

Optimal Operation of Battery Storage for Peak Shaving Applications

A Norwegian Case Study for a Medium-Scale Swimming Facility

Frida Berglund

Master of Energy and Environmental Engineering
Submission date: June 2018
Supervisor: Kjetil Uhlen, IEL
Co-supervisor: Bjørn Aas, SIAT

Norwegian University of Science and Technology
Department of Electric Power Engineering

Problem Description

With the vast implementation of power-demanding devices, the grid is facing supply challenges in terms of covering the peak power demand. One solution is to expand the existing grid, resulting in large investment costs. Another solution could be to encourage end users to reduce their power demand. Commercial users are subject to a peak demand charge, meaning they are charged for the highest peak power drawn from the grid each month. The demand charge may be high, and the resulting cost of peak power may contribute to a substantial part of the total electricity bill. As such, there is a large incentive for commercial consumers to reduce their power demand.

Sports facilities are a special type of consumer, as they tend to have a high, continuous demand with extreme peak power periods during busy hours or events. Moreover, load shifting is not always an available option. A promising solution for reducing the peak demand is battery storage, where energy can be bought from the grid to charge the battery during off-peak hours, and discharged to supply the load during on-peak hours. This is called peak shaving, and would both relieve the grid of stress and reduce the cost of peak power for the facility. With the introduction of local generation, such as from solar modules, the battery may also be charged by excess production, thus increasing self-consumption. However, due to the high investment cost of battery storage, it is important to operate the battery in a way that ensures longevity such as to avoid early re-investments.

With basis in a medium-scale swimming facility, the objective is to analyze whether implementing battery storage into the existing system can be beneficial in terms of reducing the overall system costs. The candidate shall:

- Give a brief introduction to relevant system theory, with emphasis on the battery storage system.
- Build an optimization model with the objective of minimizing the total system costs while ensuring longevity of the battery.
- Simulate the system operation and analyze whether implementing battery storage is economically profitable today.
- Conduct sensitivity analysis on important system parameters, as well as simulating the system operation for a future scenario.

Acknowledgement

This thesis concludes my final semester as a M.Sc. student at the Department of Electric Power Engineering at NTNU. The last five years have been wonderful, and I am forever grateful for the experiences I have gained from my years in Trondheim.

I would like to thank my supervisor, Professor Kjetil Uhlen, for great guidance throughout the semester. Your inputs and availability have been highly appreciated. I would also like to thank my co-supervisor, Bjørn Aas at SIAT, who has provided me with motivation and data, and then some. This thesis would not have been possible without your helpful guidance and fast responses.

A special thank you is aimed at PhD candidate Salman Zaferanlouei for helping me out with the simulation model. Your patience and expertise has saved me a lot of frustration this semester.

Lastly, I would like to express gratitude towards my friends and family for all your love and support. Especially Jarand Hole, who has provided me with heaps of moral support and interesting discussions. Completing this degree would not have been possible without you, and I am forever grateful.

Trondheim, 07.06.2018

Frida Berglund

Abstract

With the vast implementation of power-demanding devices, the grid is facing supply challenges. A promising solution could be to implement a peak demand charge, thus encouraging end users to reduce their power demand. Commercial users are already subject to this demand charge, and are billed for the highest peak power drawn from the grid each month. A special type of customer are sports facilities, as they tend to have high, continuous load demand with extreme peak power periods during busy hours or events. The resulting cost of peak power may be substantial, and contribute to a large share of the total cost of electricity. As such, there is an incentive for the facilities to reduce their power demand. However, doing so in terms of shifting the load to off-peak hours is not always an available option, as the load demand may be highly dependent on external factors. An alternative solution may be to implement battery storage, where energy is bought from the grid during off-peak hours, and discharged to supply the load during on-peak hours. This is called peak shaving, and could both relieve the grid of stress as well as reduce the cost of peak power for the facility.

In this thesis, the economic benefits of implementing battery storage into an existing grid-connected PV system for a medium-scale swimming facility is studied. The objective is to minimize the total cost of electricity, including the cost of energy and peak power demand, while ensuring longevity of the battery. The degradation of the battery is modelled as an operational cost, and is included in the objective function. An optimization model based on multi integer linear programming is built, and simulated using a one year time horizon in GAMS and Matlab. Several studies are carried out using an hourly real-time pricing scheme and data from Holmen swimming facility, however the model can easily be adapted to fit any load and production profile.

The main results reveal that installing a battery storage system is economically attractive today, with a net savings on the total system cost of 0.64% yearly. The cost of peak power is reduced by 13.9%, and the savings from peak shaving operation alone is enough to compensate for the yearly cost of the battery. Moreover, the battery ensures additional revenue by performing price arbitrage operations. The yearly degradation of the battery is found to be 7.15%, and the optimal battery size is 150 kWh. When simulating the system for an assumed 2030 scenario, the battery is found to be even more profitable with a yearly net savings of 4.15%.

Sammendrag

Med et stadig økende effektforbruk har begrensninger i overføringskapasitet blitt en stor utfordring for kraftnettet. En løsning kan være å innføre et effektledd i strømprisen for å oppfordre sluttbrukere til å redusere effekttoppene. Dette er allerede implementert hos kommersielle sluttbrukere, som blir fakturert for det høyeste effektuttaket hver måned. En interessant forbrukertype er idrettsanlegg, som er preget av kontinuerlig høye lastbehov med ekstreme effekttopper under travle besøkstider og arrangementer. Den månedlige effektkostnaden kan utgjøre en betydelig del av den totale strømregningen, og anlegget vil dermed ha økonomiske insentiver for å redusere effekttoppene. En mulig løsning kan være å implementere batteribasert energilagring, der batteriet lades opp under perioder med lav last og lades ut under topplastperioder for å dekke effekttoppene. Dette kalles for effektutjevning, og kan både avlaste kraftnettet samt redusere effektkostnadene for anlegget.

I denne oppgaven vurderes de økonomiske fordelene ved å implementere batterilagring i et nettilkoblet PV-system for en svømmehall, nærmere bestemt Holmen svømmehall i Asker. Målet er å minimere strømkostnadene, herunder kostnadene for importert energi og effekt, samtidig som batteriets levetid maksimeres. Aldringen av batteriet er i denne oppgaven modellert som en driftskostnad og inngår i objektfunksjonen. En optimeringsmodell basert på lineær heltallsprogrammering er utviklet, og simulert over ett år i GAMS og Matlab. Flere ulike case-studier er utført basert på last- og produksjonsdata fra svømmehallen, med antagelsen om en timesbasert strømpris.

Resultatene viser at installasjon av et batterilagringssystem er økonomisk gunstig allerede i dag, med en reduksjon i årlige systemkostnader på 0,64%. Effektkostnadene reduseres med 13,9% totalt, og besparelsene fra effektutjevning overgår de årlige driftskostnadene til batteriet. Videre sikrer batteriet ytterligere fortjenester ved å utnytte timesvariasjoner i strømprisen, såkalt prisarbitrasje. Den optimale batteristørrelsen er funnet til å være 150 kWh, med en årlig aldring på 7,5%. For et antatt 2030-scenario øker den økonomiske gevinsten ved å installere et batterilagringssystem ytterligere, med en årlig reduksjon i systemkostnadene på 4,15%.

Table of Contents

List of Figures

List of Tables

Acronyms

PV	✢	Photovoltaic
BESS	✢	Battery Energy Storage System
UPS	✢	Uninterruptible power supply
AC	✢	Alternating current
DC	✢	Direct current
SOC	✢	State of charge
DOD	✢	Depth of discharge
SOH	✢	State of health
NMC	✢	Nickel manganese cobalt oxide
IRENA	✢	International Renewable Energy Agency
IGBT	✢	Isolated-gate bipolar transistor
MOSFET	✢	Metal–oxide–semiconductor field-effect transistor
VSC	✢	Voltage source converter
MMC	✢	Modular multilevel converter
TOU	✢	Time-of-use
RTP	✢	Real-time pricing
LP	✢	Linear programming
SOS2	✢	Special ordered set of type 2
PR	✢	Performance ratio
GAMS	✢	The General Algebraic Modeling System
NREL	✢	The National Renewable Energy Laboratory
MILP	✢	Multi integer linear programming

1 | Introduction

1.1 Background and objective

1.1.1 Motivation and Value of Adopting Battery Storage

With an ever increasing energy demand and the introduction of more and more power demanding devices, the Norwegian grid is facing supply challenges. Especially a high power demand causes a stress on the grid, as it is dimensioned with regards to the peak power it needs to deliver. One solution would be to expand the existing grid, resulting in substantial investment costs. Another promising solution could be to implement a peak demand charge, encouraging end users to shift or reduce their power demand.

Commercial customers are already subject to a peak demand charge, and are billed for the highest peak power drawn from the grid each month. A special type of customer are sports facilities, as they tend to have high, continuous load demand with extreme peak power periods during busy hours or events. The resulting cost of peak power may be substantial, and contribute to a large share of the total cost of electricity. As such, there is a large incentive for the facilities to reduce their power demand. However, doing so in terms of shifting the load to off-peak hours is not always an available option, as the load demand may be highly dependent on external factors. An alternative solution may be to implement battery storage, where energy is bought from the grid during off-peak hours, and discharged to supply the load during on-peak hours. This is called peak shaving, and could both relieve the grid of stress as well as reduce the cost of peak power for the facility.

With the introduction of local generation, such as from solar modules, the battery may be charged by excess production, thus increasing self-consumption. These behind-the-meter applications, where the battery is paired with photovoltaic (PV) installations, is one of the most promising markets for

battery energy storage systems (BESS). It is estimated that by 2030, behind-the-meter storage could account for up to 64% of all installed capacity in stationary applications. Moreover, the investment costs are expected to fall by 50-66%, making them an attractive solution [4].

Along with being used for behind-the-meter applications, battery storage systems can also provide a wide range of services for the grid. These include, among others, frequency regulation, improved voltage quality, smoothing of renewable generation and uninterruptible power supply (UPS). Moreover, it can act as a potential source of flexibility, which is becoming an increasingly scarce resource with the vast implementation of variable generation from solar and wind. Even in the Norwegian market, where the share of fluctuating production have traditionally been low, a greater need for flexibility services is expected in the future as their share of renewables grow [8].

With more electricity coming from variable power sources, the spot marked will see more volatile prices with higher peaks and larger gaps throughout the day. If the end users are subject to an hourly pricing scheme based on the spot market, which is likely to occur in the future due to the roll-out of smart meters, implementing a BESS can provide an additional benefit in terms of price arbitrage operations. In this way, the battery charges from the grid during hours of low spot prices, and discharges to supply the load when they are higher, thus increasing its economical value.

1.1.2 Optimal Operation of Battery Storage

Even though the investment costs of batteries are expected to fall, they are still often too high for behind-the-meter applications to be economically beneficial for most customers. This, however, may often be due to over-sizing of the battery or its operation strategy being too simple. By optimally sizing and controlling the battery storage system to fit its application purposes and system specifications, the battery can minimize its operational costs while maximizing economical benefits for the customer.

Several papers have studied the optimal operation of batteries for behind-the-meter applications, and a variety of different optimization models have been carried out depending on the complexity of the problem and the desired results. Dagdougui et. al [9] used a rule-based algorithm, where the aim was to find the optimal size of the BESS which maximized annual benefits when used for

peak shaving. The model is however very simple, excluding the operational costs of the battery and running an on-peak/off-peak circuit, resulting in no profitable solutions. Dufo-López [10] also used a rule-based algorithm and real-time pricing to decide whether the gain from operating the battery at a given time step exceeded the operational costs of the battery. The goal was to minimize the net present cost of the battery, however no profitable solutions were found. Nottrott et. al [11] used linear programming and forecast algorithms to optimally schedule a battery with regards to keeping the net load demand under a pre-set power limit. Although proving more beneficial than running the battery on an on-off-mode, the optimization model is very simple.

1.1.3 The Importance of Considering Battery Degradation

None of the papers described above consider the impact of battery degradation in their solution. If the lifetime of the battery is studied, it is done after the optimal solution is found and the calculations are largely simplified. This is true for many studies, where the lifetime of the battery is often considered to be constant regardless of how it is operated. However, the operational patterns of a battery can greatly affect its degradation process, and if run too aggressively its lifetime can be considerably reduced. A reduction in lifetime will in turn create a need for early re-investments, which is largely unfavourable due to the high investment costs of battery storage. As such, measures taken to ensure longevity of the battery could potentially lead to a higher revenue for the customer in the long run.

A few papers studying the optimal operation of battery storage include degradation models in their work. Hesse et. al [12] propose a linear optimization method for cost-optimal sizing of a BESS, considering both minimizing the electricity costs and maximizing revenue generation. The degradation of the battery is modelled as an operational cost, however the aging model is simple and the effects of power peaks are neglected. Abdulla et. al [13] propose a stochastic dynamic programming technique to optimally operate a BESS, integrating both load forecast and battery degradation models. The results show that an optimally operated BESS increases the lifetime of the battery by 160%. However, no economics are included, and the peak demand charges are neglected. Ranaweera et. al [5] use dynamic programming to optimize the daily operational cost, including the cost of electricity and battery degradation. A time-dependent energy tariff is considered, however the simulation is only carried out for 24 hours, and as such the capacity of the battery is considered constant regardless of

the aging. Moreover, the peak demand charges are neglected.

1.1.4 Objective

In light of the shortcomings of the aforementioned publications, this thesis aims to build a more comprehensive optimization model, considering both the degradation of the battery and the cost of peak power. With basis in a medium-scale swimming facility, the main goal is to analyze whether implementing battery storage into an existing system can be beneficial in terms of reducing the overall system cost. The objectives of this thesis include:

- Giving a brief introduction to relevant system theory, with emphasis on the battery storage system.
- Building an optimization model with the objective of minimizing the total system costs while ensuring longevity of the battery.
- Simulating the system operation and analyzing whether implementing battery storage is economically profitable today.
- Conducting sensitivity analysis on important system parameters, as well as simulating the system operation for a future scenario.

1.2 Approach

The system model is built using mathematical equations and constraints, based on component theory. The resulting multi integer linear optimization problem is written in The General Algebraic Modeling System (GAMS) and solved using Gurobi. Data on the load demand and solar production for the test case are collected using Gurusoft®, with access provided by the swimming facility under study, and loaded to GAMS using functions in Matlab. The simulation results obtained from running the optimization in GAMS are read back to Matlab and further manipulated, in order to make the results presentable in the form of plots and graphs.

1.3 Limitations

In order to keep the scope of this thesis within reasonable boundaries, some simplifications have been made. Firstly, the BESS is simplified to contain only a battery and an inverter, hence the effects of all other system components are neglected. Furthermore, the load and production data from the swimming facility are assumed known prior to solving. As such, a perfect forecast model is assumed. However, forecasting algorithms can easily be implemented in the model, and could be of interest for future studies. Other suggestions for further work are mentioned in Section 8.1.

1.4 Structure of the Report

This thesis starts off with a brief introduction to the proposed system and the characteristics of its most important components, with emphasis on the battery storage system. This is done to present the reader with the basic knowledge necessary for understanding the working principles of the system. In this way, little previous knowledge of the terms and subjects presented in the study is required prior to reading.

Chapter 2, *A Grid-Connected Photovoltaic System with Battery Storage*, gives an introduction to the component theory and important aspects of the system. Emphasis is put on the battery storage system, with a thorough explanation of the battery degradation.

In Chapter 3, *Mathematical Formulation of the Problem*, a mathematical model of the system is presented. Moreover, the optimization model is built.

Chapter 4, *Holmen Swimming Facility*, gives a brief introduction to the main characteristics of the facility under study.

Chapter 5, *Solution Method*, explains how the optimization model is implemented using available commercial software, and how important system parameters are decided.

In Chapter 6, *Case Study Results*, the main results obtained from simulating the optimization model are presented, along with the results from sensitivity analyses and a future scenario.

In Chapter 7, *Discussion*, the main findings from the results are discussed.

Lastly, Chapter 8, *Conclusion*, summarizes and concludes the main aspects of the study, along with shortcomings and suggestions for further work.

2 | A Grid-Connected Photovoltaic System with Battery Storage

This chapter gives an introduction to the component theory and important aspects of the system, so as to give the reader an understanding of its basic working principles and to lay a foundation for building the optimization model. The system under study can be modelled simply as a grid-connected photovoltaic (PV) system supplying a load. The main goal of this thesis is to see whether introducing a battery energy storage system (BESS) can be beneficial in terms of reducing the overall cost of electricity, while accounting for the operational cost of the battery.

When connecting a BESS to the system, two different configurations can be found: direct (DC) and alternate current (AC) coupled systems [14]. In DC coupled systems, the batteries are connected to the DC link of the PV system directly or through a bi-directional converter if the battery is to be charged from the grid. In contrast, AC coupled batteries are connected to the AC bus through a charge regulator and bi-directional converter. For this study, an AC coupling of battery storage is chosen as it is suitable for the retrofitting of existing PV installations and offers flexibility in system design [15].

A simplified single-line diagram of the proposed system with its most important components is shown in Fig. 2.1. It should be noted that the BESS is simplified to contain only a battery bank and a bi-directional converter, and the effects of all other storage components are neglected in this study. The following sections give an introduction to the system components, as well as important aspects relevant for building the optimization model. Seeing as this thesis is largely concerned about battery operation, only a brief introduction of the other components will be given. Moreover, the load is first presented in Chapter 4 and is not discussed here.

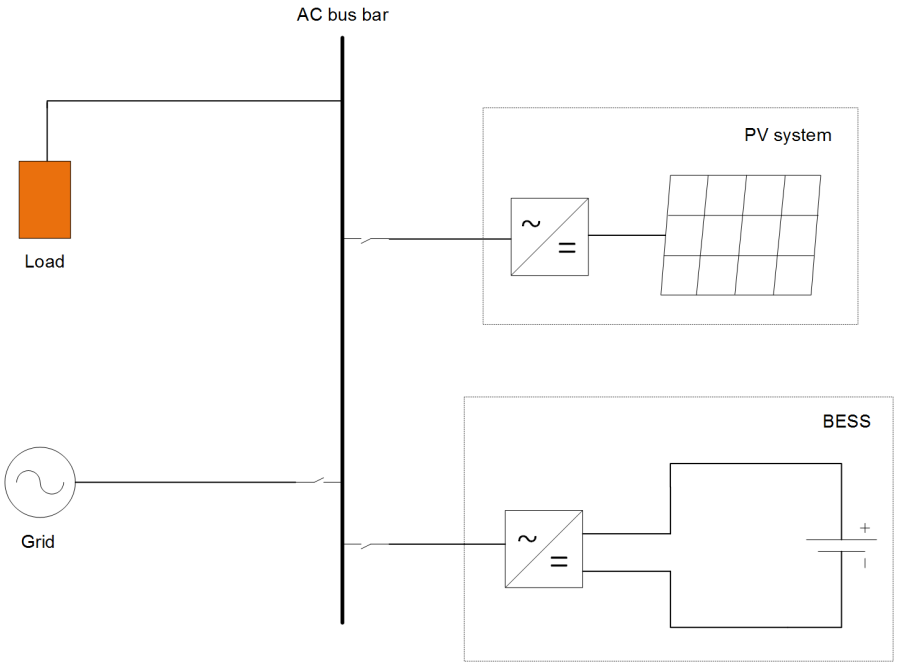

Figure 2.1: The proposed system

2.1 Battery Energy Storage Systems

A BESS consists of several components, the main one being the battery bank. The other components control the power flowing to and from the bank, typically including monitoring and control systems, power electronics like DC switch and AC breakers, and a power conversion system [16]. The battery bank consist of several batteries connected together, and its performance is strongly affected by the nature of the batteries. The different battery technologies available on the market vary greatly in their characteristics, and are therefore suited for different applications: while some batteries are powerful but costly, others are cheap but short-lived. As such, it is important to classify the main features needed before deciding on a specific technology. Table 2.1 gives an overview of the most important battery aspects, based on [17].

For behind-the-meter storage systems, where the BESS is often paired with small-scale solar PV systems and used for increased self consumption, load leveling or peak shaving, lithium-ion batteries are by far the dominant battery technology of choice ([18], [4]). When compared to other technologies, they have the advantage of high energy and power density, making them ideal for both the electromobility market and small-scale storage systems where size and weight are crucial factors.

Table 2.1: Important battery concepts

Term	Unit	Description
Capacity	Ah, kWh, MWh	The maximum amount of energy that can be stored in the battery.
State of charge (SOC)	Ah, kWh, MWh, %	The amount of energy stored in the battery at any given time. Often given as a percentage of the capacity.
Depth of discharge (DOD)	%	The amount of discharged capacity at any given time, i.e. the inverse of SOC. The deeper the DOD, the shorter the expected cycle life.
State of health (SOH)	%	The amount of capacity available in a battery relative to its starting conditions.
Round-trip efficiency	%	The efficiency of which the battery is charged and discharged, i.e. the fraction of energy coming into the battery that can be retrieved.
Cycle life	Number of cycles	The number of charge and discharge cycles a battery can complete before losing considerable performance.
Calendar lifetime	Years	The number of years a battery can operate before losing considerable performance.
Energy density	Wh/kg	Energy stored per kilogram.

They also have the ability of high power charge and discharge, as well as an excellent round-trip efficiency and low self-discharge rate [17]. Moreover, their costs are rapidly declining: in Germany, the cost of small-scale li-ion systems fell by over 60% between 2014 and 2017. Benefiting from the massive growth of electric vehicles worldwide, the cost of stationary li-ion applications are expected to decrease by another 55% by 2030 [4].

However, there is one initial drawback of lithium-ion batteries: their cycle life. Depending on the cell chemistry, it can be as low as 500 full equivalent cycles[1]. A battery of this design performing one full cycle each day would last short of one and a half years before needing replacement. Considering their high investment cost, this would not be economically viable. As such, the degradation of a battery is an important aspect to consider when deciding on its operational patterns such as to avoid excessive cycling an the need for early re-investments.

[1] A full equivalent cycle is charging the battery from its maximum to its minimum DOD, before fully emptying it again.

2.1.1 Battery Degradation

The nature of a battery is such that its usable capacity decreases as it ages. The state of health (SOH) of a battery is a measure of the current available capacity, given as a percentage of the nominal capacity. When it drops below a certain value, the battery is considered at the end of its lifetime and needs to be replaced. For lithium-ion batteries this value is normally set to 80% of the nominal capacity, matching a typical replacement criteria for electric vehicles. However, this end-of-life threshold can vary depending of the battery chemistry, user preference and application area.

To estimate the SOH of a battery, either an analytical or a measurement based model can be used. For lithium-ion batteries, it is common to differentiate between two factors influencing the SOH; cyclic and calendric aging [19]. Cyclic aging is the degradation of a battery due to the battery going through a full charging cycle, while the calendric aging is the inevitable time-dependant capacity loss occurring regardless of operation. In addition, the aging of a battery is influenced by several operating factors, such as inefficient charging, high charging voltages and currents, deep discharging and extreme temperatures [5].

2.1.1.1 Cyclic Aging

Cyclic aging is caused by energy throughput in the battery, and for each cycle the battery goes through, a certain percentage of available capacity is lost. The amount of capacity lost during a cycle is highly dependant on the cell chemistry, and the various operating factors affect the battery chemistries differently. For most lithium-ion batteries, the available capacity is sensitive to both the maximum number of full cycles and the depth of discharge (DOD) level of each cycle [20]. Fig. 2.2 shows the number of cycles versus DOD for a nickel manganese cobalt oxide (NMC) battery, a commonly used storage chemistry for small-scale behind-the-meter applications. The figure is based on references [1] and [2] where a least square fitting method was applied to test data. The data was acquired by repeatedly discharging the battery from full capacity to a specified DOD level, called a regular cycle, and noting the number of cycles the battery could go through before reaching its end of life capacity.

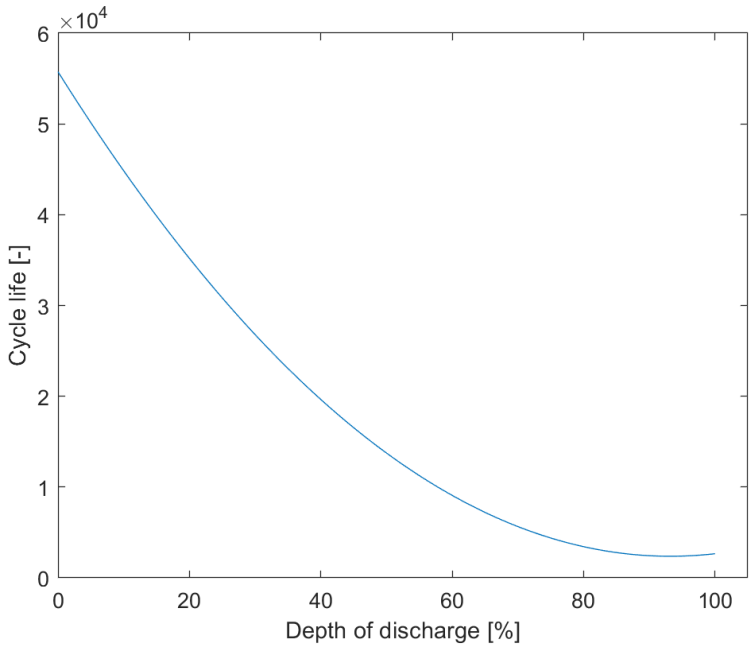

Figure 2.2: Cycle life versus DOD for a NMC battery, based on data from [1] and [2]

However, a battery is not always operated using regular cycles. This is especially true for behind-the-meter applications, where the battery operation is largely dependent on signals received from outer factors such as the energy price, power demand and local power production. Seeing as these signals may vary greatly from one period to another, the battery will largely go through irregular cycles [1]. It is therefore necessary to build a cyclic degradation model which reflects the irregular behaviour of the battery.

Modelling the cyclic aging of a battery is difficult as it depends on both the energy throughput, cell chemistry and operating conditions, such as temperature, cell voltage and DOD. As such, no single model can be used for all chemistries, and a near accurate representation of the cyclic aging for each chemistry would be a highly non-linear function. As such, several simplified methods have been proposed. In one article by Yang et. al [3], the cyclic degradation was found by measuring the amount of coulombs through a battery for each full cycle and comparing it with the available amount. A constant capacity reduction rate was assumed in order to simplify the analysis, meaning the SOH decreased linearly with the number of cycles. However, the study only accounts for regular cycles. Andre et. al [21] used a dual filter consisting of a standard Kalman filter and an Unscented Kalman filter to predict the internal states of the battery and thus the total degradation. Although producing accurate results, this method is both complex and time consuming.

Other articles ([1], [22]) propose a simpler model for calculating the cyclic aging using the curve from Fig. 2.2: the degradation of each regular cycle, i.e. when discharging the battery from full capacity to a specified DOD level, is modelled as seen in Eq. (2.1). L_{cyc} is the cycle life of the resulting DOD and ρ is the percentage degradation. Although being cell specific, it can easily be adapted to fit all chemistries where such a curve is available, and can therefore produce accurate results for the chosen battery technology.

$$\rho = \frac{100\%}{L_{cyc}} \tag{2.1}$$

As previously mentioned, it is desirable to build a model which accounts for irregular battery cycles. In a paper by Wang et. al [1], an irregular cycle is modelled as the difference between two regular cycles, as seen in Eq. (2.2). Here, DP_{cyc} represents the degradation in each time period. The absolute value is due to the fact that both charging and discharging contributes to a degradation of the battery, and the factor of 0.5 reflects that one charging or discharging process contributes to half of the degradation of a full cycle. For example, if the battery is charged from 80% DOD to 20% DOD during one period, the degradation percentage is equal to $0.5 \cdot |1/3221 - 1/34917| = 0.014\%$.

$$DP_{cyc} = 0.5 \cdot |\rho_t - \rho_{t-1}| \tag{2.2}$$

2.1.1.2 Calendric Aging

As opposed to cyclic aging, calendric aging is independent of energy throughput and comprises all internal processes leading to the degradation of a battery when idle. The capacity lost during these idle intervals is mainly dependent on the storage state of charge (SOC) and temperature. Several papers ([3], [23]) have studied the change in the SOH for lithium-ion batteries when storing them at different temperatures and SOCs, and found that the calendric aging did not increase linearly with the SOC, nor with temperature. This can be seen in Fig. 2.3, taken from [3], showing the capacity loss per day as a function of temperature for a lithium ferrophosphate (LFP) battery for different levels of SOC.

Trying to create a mathematical model for the calendric aging based on this figure would require different equations for different temperatures, making the model complex. However, assuming a

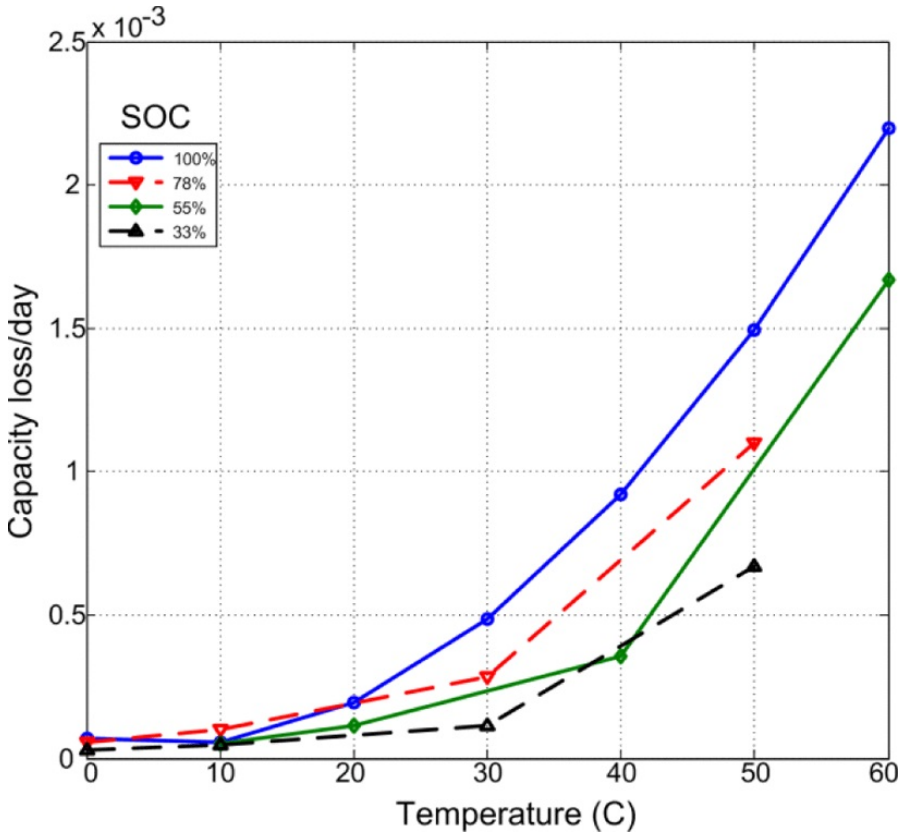

Figure 2.3: Capacity loss as a function of temperature for different levels of SOC, taken from [3]

constant temperature can simplify the model. A constant temperature can be obtained by ensuring a stable climate for the battery storage system, such as installing it indoors and providing a cooling system if necessary. With this in mind, the calendric aging of the battery can be modelled as:

$$DP_{cal} = a \cdot SOC^2 + b \cdot SOC + c \tag{2.3}$$

where DP_{cal} is the degradation in each period, and a, b and c are constants depending on the chosen temperature [3]. Seeing as the storage SOC is not constant - in fact, it changes with each cycling of the battery - Eq. (2.3) is a non-linear equation. Several papers ([12], [24]) propose a further simplification: a solely time-dependent model of the calendric aging. Here, the degradation in each time step is expressed as:

$$DP_{cal} = \frac{100\%}{L_{cal}} \tag{2.4}$$

where L_{cal} is the shelf time[2] of the battery given by the manufacturer. This simplification can be

[2]The estimated lifetime of the battery if no charge throughput is applied, i.e. when idle.

justified when assuming a constant, low temperature (10 or 20°C): when looking at Fig. 2.3, it can be seen that the capacity loss for different levels of SOC is approximately equal for these temperatures.

2.1.1.3 Total Aging

As previously mentioned, both the cyclic and calendric aging affect the SOH of the battery. With the total degradation expressed as DP, the battery is at the end of its lifetime for DP = 100%. If the end-of-life criterion is set to 80% of full capacity, the SOH of the battery in each period can be modelled as seen in Eq. (2.5), where DP_t is the total degradation in per unit in time period t.

$$SOH_t = SOH_{t-1} - 0.2 \cdot DP_t \tag{2.5}$$

According to the state of the art, the total degradation of the battery can be modelled in several ways. Some articles ([12], [25]) model the total aging as a superposition of the cyclic and calendric aging, while others ([3], [5]) argue that the two processes are independent of each other: the total aging is equal to DP_{cyc} if the battery is operating, and DP_{cal} if it is idle, as seen in Eq. (2.6):

$$DP = \begin{cases} DP_{cal}, & P_{charge} = P_{disch} = 0 \\ DP_{cyc}, & otherwise \end{cases} \tag{2.6}$$

Other articles again ([1], [24]) argue that the total degradation in each period can be modelled as the larger one of the two aging processes. If DP_{cyc} is higher than DP_{cal} for all DOD levels, and noting that DP_{cal} is equal to zero when the battery is idle, this approach can be seen as a simplification of Eq. (2.6). The resulting model is shown in Eq. (2.7).

$$DP = \max\{DP_{cyc}, DP_{cal}\} \tag{2.7}$$

2.1.2 The Cost of Battery Storage

As previously mentioned, the degradation of the battery is an important factor to consider when optimizing the battery operation. Excessive cycling of the battery is unwanted as this will decrease the battery lifetime, potentially drastically. The battery should only be operated if the cost of capacity loss during cycling is less than the economic savings from supplying the load with the battery instead of buying from the grid. However, there is also a cost of keeping the battery idle, namely

the gradual degradation due to calendric aging, which needs to be accounted for. The degradation cost in each period is thus dependent on the total degradation of the battery. By assuming that the degradation cost is a percentage of the initial investment cost, such that when the battery reaches the end of its lifetime the initial investment is accounted for, the degradation cost can be expressed as follows [22]:

$$\gamma = C_{bat} \cdot DP \tag{2.8}$$

where C_{bat} is the initial cost of the battery. The initial cost is highly dependent on the size of the battery, as seen in Eq. (2.9) where c_{bat} is the specific cost in NOK per capacity and E_{bat}^{nom} is the nominal capacity of the battery.

$$C_{bat} = c_{bat} \cdot E_{bat}^{nom} \tag{2.9}$$

As seen from these equations, the degradation cost of the battery is strongly affected by the initial investment cost, which in turn varies greatly for each cell chemistry: today's average prices for a BESS can range from NOK 2800 to NOK 8400 per kWh[3]. However, with increasing deployment of li-ion batteries in various applications worldwide, costs are rapidly declining: in a study by the International Renewable Energy Agency (IRENA) from 2017 [4], average battery system costs are expected to lie between NOK 1000 and NOK 2800 per kWh in 2030, a reduction of around 55% from today's prices [4]. These estimations are further backed up by Bloomberg New Energy Finance [26]. Moreover, continued improvement in technology will increase the performance and cost competitiveness of li-ion batteries, and especially their lifetime is expected to improve drastically: by 2030, the cycle lifetime of some cell designs could increase by as much as 90%. Fig. 2.4, taken from [4], gives an overview of the current and projected properties of some important li-ion battery storage systems, with the dots indicating the average, or central, estimates.

[3]Based on conversion from USD to NOK, with a exchange rate of 8.00 NOK/USD.

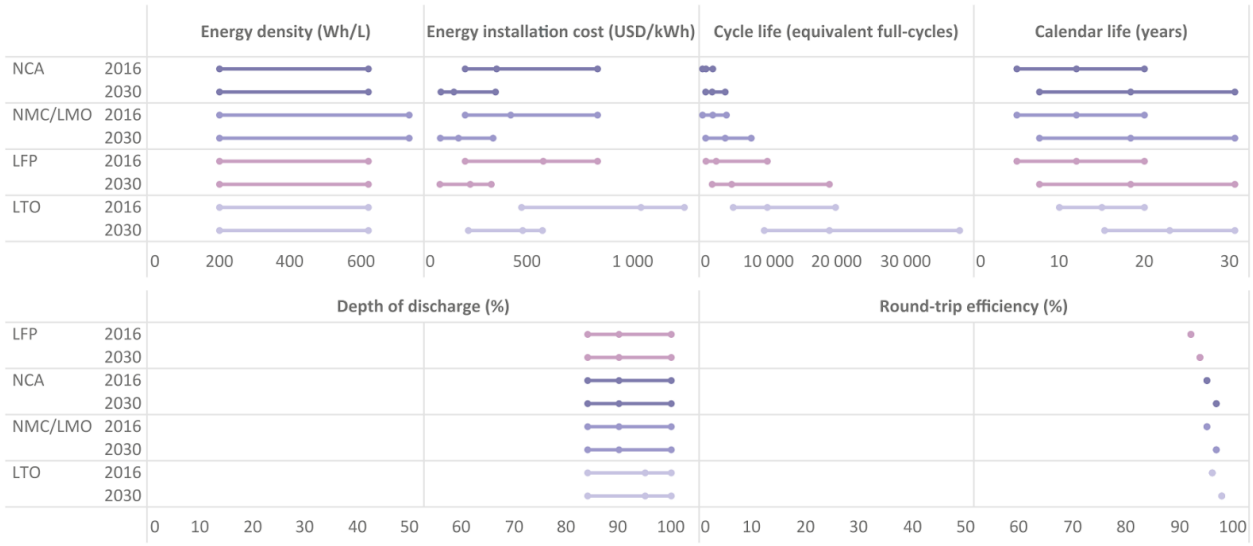

Figure 2.4: Current and projected properties for some important lithium-ion BESS, taken from [4]

2.1.3 The Battery Inverter

The following two paragraphs are extracts from the preceding specialization project, reference [27]. It should be noted that the words converter and inverter are used interchangeably throughout this study when referring to the bi-directional converter of the BESS.

A power converter is an electronic device which controls and modifies the voltage and current to desired values. In its simplest form it consist of several passive elements (capacitor, inductor, diode, thyristor), but it can also contain controllable switches (IGBT, MOSFET). Due to the large number of possible combinations, there are many different converter topologies on the market.

The battery converter transforms AC power from either the grid or the solar inverters to DC power when charging, and from DC to AC power when discharging, meaning it acts as a bi-directional converter. Its size can vary depending on the application, however it is typically matched to provide the nominal power of the battery. The topologies commonly used for BESS are two- or three-level voltage source converters (VSC), however the more complex modular multilevel converter (MMC) may also be a good choice. Although more costly than the conventional VSC, it offers several advantages like low harmonic distortion, superb efficiency and high scalability and reliability. The efficiency of the converter depends on the topology, however it commonly lies in the range between 90% - 98% [28].

The cost of the inverter is included in the total cost of the BESS from Section 2.1.2, and is thus not

discussed further.

2.2 The PV System

A PV system is designed to supply loads with solar power, and is made up of several PV modules wired together. These modules are in turn a number of series-connected solar cells, where each cell produces electricity when exposed to sunlight. The system also commonly includes a power converter, which converts the DC output from the solar panels to usable AC input for the loads.

By installing a PV system, the amount of power bought from the grid is reduced as the electricity produced by the solar panels are used to supply the loads. If the solar production exceeds the load demand at any point, the excess power is fed back to the grid. The owner of the PV system is compensated for each kWh of energy sold to the grid by a feed-in tariff. This is known as the "plus customer scheme", and is a means of compensating prosumers[4] for power delivered to the grid as long as this never exceeds 100 kW [29]. However, with the vast deployment of PV systems compensation becomes increasingly expensive, and hence the feed-in tariffs are likely to decrease in the near future. With the inclusion of a BESS, the excess power can be used to charge the battery bank. When the net load demand[5] is high, the battery can be discharged to supply the load, thus increasing self-consumption.

2.3 The Grid

The electrical grid is a network through which the power generated at the producer level is transmitted and distributed to the end users. Each user, or consumer, is charged for the power delivered, and the electricity bill normally consists of two parts [30]:

- The grid rent, comprising a fixed and variable amount. This rent is charged by the local network company, and covers all cost related to transferring the energy.
- The price of electricity, which is the cost of the total amount of energy bought from the local power supplier in each billing period.

[4] Customers who both consume and produce power
[5] The solar power production subtracted from the load demand

Each kWh of energy delivered is subject to an energy tariff, which can be either a flat rate or a time-dependant rate. With the flat rate tariff, the customer is charged a constant price for each kWh consumed, which may or may not be seasonal dependant. Traditionally, the flat rate is the most widespread tariff scheme in Norway. However, with the introduction of smart meters[6] the consumers will be more exposed to price signals in the power market, and time-based tariffs may become increasingly deployed. Instead of charging a constant price, the cost per kWh is dependant on the time in which that kWh is used. The two most common time-based tariff schemes are:

- Time-of-use pricing (TOU): The energy tariff is divided into time periods, with fixed electricity prices within each period. The prices are higher during peak periods to encourage customers to reduce their load demand, thus relieving the grid of high stress.
- Real-time pricing (RTP): The energy tariff is based on hourly rates, which depend on the spot prices. In Norway these are decided by Nord Pool[7].

In addition to being charged for both the grid rent and the total energy consumed, commercial customers like swimming facilities are subject to a demand charge - a fee charged for the maximum power drawn from the grid each billing period. This charge may be of a substantial amount, and is set high to reflect that the consumption peaks cause a stress on the grid. For some customers, the peak demand charge could be as high as their cost of energy, and flattening the peak demand may thus be an efficient way of reducing their total electricity bill. This can be done by implementing a BESS, where the battery is charged during off-peak hours and discharged during hours of high load to shave the peaks.

Under a time-based tariff scheme the economic value of storage systems is further increased, as they may be used for price arbitrage operations: the battery is charged from the grid when the price of electricity is low, and discharged to supply the load when the price is high. This is especially beneficial for areas where the difference between on and off-peak energy tariffs are high, which may be the case for Norway in the near future: according to a study made by Statnett this year [8], the Norwegian spot market will see more volatile prices and higher price peaks as the implementation of fluctuating power sources like solar and wind continue to grow. If a RTP scheme is introduced, which may be

[6]Smart meters measure the hourly consumption for each customer, and sends this information to the network company.

[7]Nord Pool runs the leading power market in Europe, and offers day-ahead and intraday markets. The day-ahead market is the main arena for trading power, and the intraday market helps secure balance between supply and demand [31].

likely due to the vast roll-out of smart meters, a BESS can exploit these large price variations and provide additional savings. Moreover, implementing a BESS in connection with the grid can provide other benefits: seeing as the power output of renewable resources can vary greatly depending on the weather, and since supply and demand need to be balanced in real time, a greater need for flexible solutions is expected in the future. With a BESS, the battery can store the electricity generated when production exceeds demand, and supply electricity when needed, thus effectively smoothing the variable production and ensuring quality of supply. However, as this thesis is concerned with behind-the-meter applications and customer benefits, this topic is not discussed further.

2.3.1 The Total Cost of Electricity

The total cost of electricity for each billing period can be modelled as shown in Eq. (2.10), where t indicates hours and T is the last hour of the billing period. $c_{el,t}$ is the energy tariff, $c_{feed\text{-}in,t}$ is the feed-in tariff, and c_{peak} is the peak demand charge. $P_{grid,b,t}$ is the power bought from the grid each hour, $P_{grid,s,t}$ is the power fed back (or sold) to the grid each hour, and P_{peak} is the maximum amount of power drawn from the grid during the billing period.

$$C_{el} = \sum_{t}^{T} (c_{el,t} \cdot P_{grid,b,t} \Delta t - c_{feed-in,t} \cdot P_{grid,s,t} \Delta t) + c_{peak} \cdot P_{peak} \tag{2.10}$$

3 | Mathematical Formulation of the Problem

The single-line diagram of the proposed system is reproduced in Fig. 3.1 for convenience, along with the power flows. All power flows going into the AC bus are considered positive.

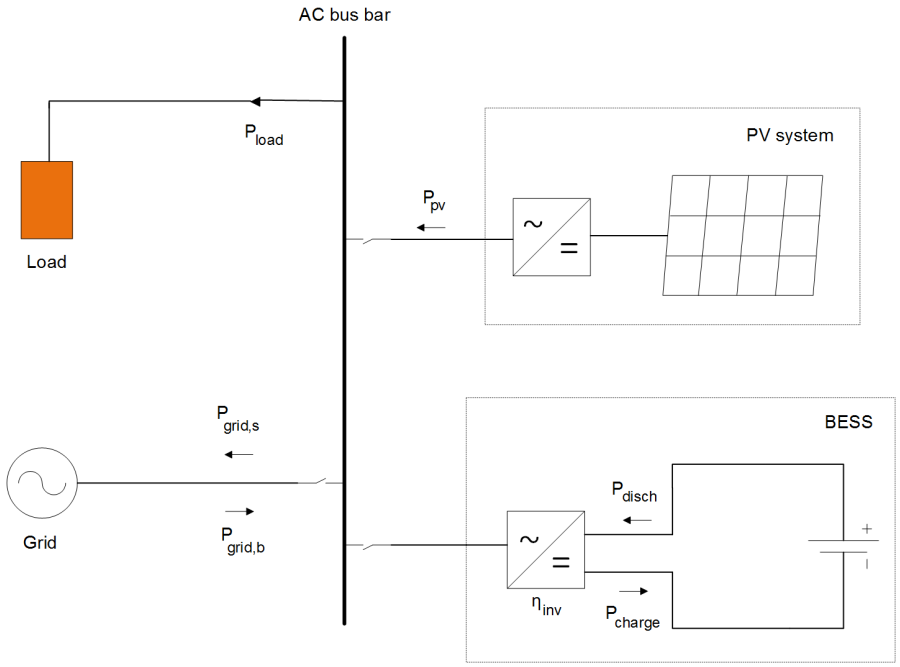

Figure 3.1: The proposed system with power flows

3.1 Assumptions

The following assumptions have been made on the system characteristics in order to simplify the problem:

- The hourly load demand and solar production are assumed to be known prior to solving the problem, meaning we have a perfect forecast model which greatly simplifies the problem. Although not a part of this study, forecasting algorithms can easily be implemented in the model in order to produce more realistic results.
- The battery is based on the characteristics of a lithium-ion NMC battery.
- The C-rate of the battery is assumed equal to one, meaning the battery can charge or discharge all available energy in one hour within the limits of the BESS inverter. This is chosen based on the typical ratings of a NMC battery [32].
- All efficiencies are assumed to be constant.

3.2 Notations

Sets

T	-	Set of time periods, $t \in$ T
M	-	Set of months, $m \in$ M
I	-	Set of piecewise linear points, $i \in$ I

System parameters

Δt	-	Time resolution [h]
$P_{load,t}$	-	Load demand [kW]
$P_{pv,t}$	-	Solar production [kW]
P_{grid}^{max}	-	Maximum power that can be bought from the grid [kW]
P_{inv}^{nom}	-	Nominal power of the BESS inverter [kW]
η_{inv}	-	Efficiency of BESS inverter [-]
η_{charge}	-	Charging efficiency of the battery [-]
η_{disch}	-	Discharging efficiency of the battery [-]

η_{rt}	-	Round-trip efficiency of the battery [-]
E_{bat}^{nom}	-	Nominal battery size [kWh]
SOC_{min}	-	Minimum state of charge [p.u.]
SOC_{max}	-	Maximum state of charge [p.u.]
L_{cal}	-	Calendric lifetime of the battery [h]

Economic parameters

$c_{el,t}$	-	Energy tariff [NOK/kWh]
$c_{feed\text{-}in,t}$	-	Feed-in tariff [NOK/kWh]
$c_{peak,m}$	-	Peak demand tariff [NOK/kWp/month]

System variables

$P_{grid,b,t}$	-	Power bought from the grid [kW]
$P_{grid,s,t}$	-	Power sold to the grid [kW]
$P_{peak,m}$	-	Peak power demand [kWp]
$P_{charge,t}$	-	Power charged to the battery [kW]
$P_{disch,t}$	-	Power discharged from the battery [kW]
$E_{bat,t}$	-	Energy content in the battery [kWh]
$E_{bat,t}^{usable}$	-	Usable capacity [kWh]
SOC_t	-	Battery state of charge [p.u.]
DOD_t	-	Battery depth of discharge [p.u.]
SOH_t	-	Battery state of health [p.u.]
DP_t	-	Total battery degradation [p.u.]
$DP_{cyc,\ t}$	-	Cyclic degradation [p.u.]
$DP_{cal,\ t}$	-	Calendric degradation [p.u.]
ρ_t	-	Cyclic degradation of a regular cycle [p.u.]
γ_t	-	Cost of degradation [NOK]

Variables used for piecewise linearization

$deg_{t,i}$	-	Degradation in point i [p.u.]
$dod_{t,i}$	-	DOD in point i [p.u.]
$w_{t,i}$	-	SOS2 variable [-]

3.3 Mathematical Model

The most important aspect of the system is to ensure that the load demand is met at all times, and that the power balance is obtained. As can be seen from Fig. 3.1, the power balance equation in time step t can be written as:

$$P_{pv,t} + P_{grid,b,t} + \eta_{inv} P_{disch,t} = P_{grid,s,t} + \frac{P_{charge,t}}{\eta_{inv}} + P_{load,t} \tag{3.1}$$

Both the PV production and load demand are given as parameters, while the battery charging and discharging power as well as the power bought from or sold to the grid are variables. In order to reduce the power peaks as seen from the grid, and thus enable peak shaving, a maximum limit on the power that can be drawn from the grid in any time step is applied:

$$P_{grid,b,t} \leq P_{grid}^{max} \tag{3.2}$$

Moreover, both the power bought from and sold to the grid must be of positive values:

$$P_{grid,b,t}, P_{grid,s,t} \geq 0 \tag{3.3}$$

3.3.1 Modelling the Battery

When the battery is operating, it can either charge or discharge - but never both at the same time. In each time step, the charging or discharging powers are limited by the nominal power of the bi-directional inverter to avoid over-voltages and high currents:

$$0 \leq P_{charge,t} \leq \eta_{inv} \cdot P_{inv}^{nom} \tag{3.4}$$

$$0 \leq P_{disch,t} \leq P_{inv}^{nom} \tag{3.5}$$

In each operating period, the energy in the battery is either increased or reduced according to Eq. (3.6). Note that when the battery is idle, $P_{charge,t} = P_{disch,t} = 0$ and the energy content remains unchanged.

$$E_{bat,t} = E_{bat,t-1} + \eta_{charge} \cdot P_{charge,t}\Delta t - \frac{P_{disch,t}}{\eta_{disch}}\Delta t \tag{3.6}$$

The charging and discharging efficiencies depend on the current through the battery, however for simplification they are assumed constant throughout the simulation. Furthermore, it is assumed that the efficiencies are equal, and that they can be calculated based on the battery round-trip efficiency (η_{rt}) ([5], [10], [12]):

$$\eta_{charge} = \eta_{disch} = \sqrt{\eta_{rt}} \tag{3.7}$$

The energy content in the battery is limited by an upper and lower boundary, as given in Eq. (3.8), to avoid overcharge or deep discharge:

$$E_{bat,t}^{usable} \cdot SOC_{min} \leq E_{bat,t} \leq E_{bat,t}^{usable} \cdot SOC_{max} \tag{3.8}$$

The available energy is controlled by the usable capacity as well as the minimum and maximum levels of the state of charge (SOC_{min} and SOC_{max}), which are set according to Fig. 3.2.

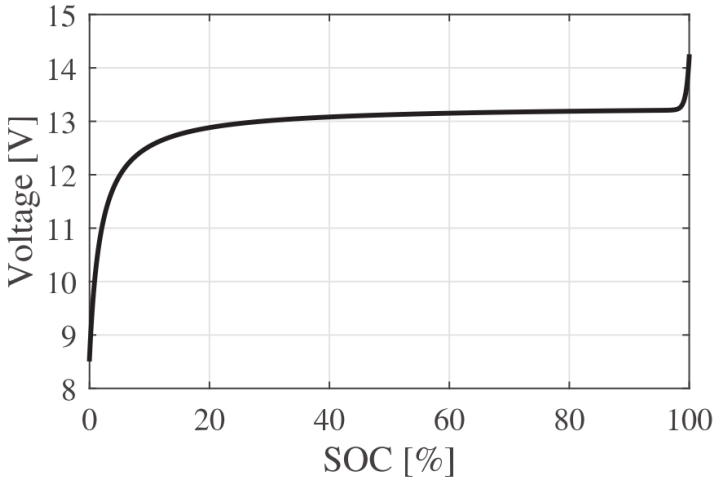

Figure 3.2: Open circuit voltage as a function of SOC for a lithium-ion battery, taken from [5]

From the figure it can be seen that the open circuit voltage of a lithium-ion battery is relative constant

in the SOC range of 10% - 90%, so operation in this region is preferable [5]. Moreover, as discussed in Section 2.1.1, the battery deteriorates due to calendric and cyclic aging processes. As such, the usable capacity, $E_{bat,t}^{usable}$, decreases with each time step according to the state of health (SOH_t). The resulting limits on the energy content are shown below:

$$E_{bat}^{nom} \cdot SOH_t \cdot SOC_{min} \leq E_{bat,t} \leq E_{bat}^{nom} \cdot SOH_t \cdot SOC_{max} \tag{3.9}$$

The SOC and the energy of the battery are interdependent, and the SOC can be expressed as:

$$SOC_t = \frac{E_{bat,t}}{E_{bat,t}^{usable}} = \frac{E_{bat,t}}{E_{bat}^{nom} \cdot SOH_t} \tag{3.10}$$

In addition, as previously mentioned, the SOC is limited to its minimum and maximum levels:

$$SOC_{min} \leq SOC_t \leq SOC_{max} \tag{3.11}$$

The DOD of the battery is dependent on the SOC, and vice versa, and is defined as:

$$DOD_t = 1 - SOC_t \tag{3.12}$$

3.3.1.1 Battery Degradation

The degradation of the battery was described in Section 2.1.1, however the equations used in the simulations are reproduced here for convenience. Considering the battery to be at the end of its lifetime when its capacity is reduced by 20%, the SOH in each time step can be modelled as:

$$SOH_t = SOH_{t-1} - 0.2 \cdot DP_t \tag{3.13}$$

where DP_t is the total degradation in each time step, given as:

$$DP_t = \max\{DP_{cyc,t}, DP_{cal,t}\} \tag{3.14}$$

The cyclic and calendric aging models used in this study are shown below:

$$DP_{cyc,t} = 0.5 \cdot |\rho_t - \rho_{t-1}| \tag{3.15}$$

$$DP_{cal,t} = \frac{100\%}{L_{cal}} \tag{3.16}$$

where ρ_t is modelled as seen in Eq. (2.1) from Section 2.1.1.1. The calendric aging model was chosen based on its simplicity and linearity as compared to the other models presented in Section 2.1.1.2.

3.3.2 The Objective Function

The objective of the model is to minimize the total system cost while satisfying the constraints described above. The system cost consists of two parts: the total cost of electricity, and the operational cost of the battery. The operational cost of the battery is assumed to only include the cost of degradation, hence maintenance costs are neglected.

Based on Eq. (2.10) from Section 2.3.1, the total cost of electricity can be modelled as:

$$C_{el} = \sum_{t \in T} (c_{el,t} \cdot P_{grid,b,t} \Delta t - c_{feed-in,t} \cdot P_{grid,s,t} \Delta t) + \sum_{m \in M} (c_{peak,m} \cdot P_{peak,m}) \tag{3.17}$$

where $P_{peak,m}$ is the maximum power drawn from the grid in time t within month m, given as:

$$P_{peak,m} \geq P_{grid,b,t} \quad \forall t \in M \tag{3.18}$$

The total degradation cost of the battery can in turn be modelled as:

$$C_{deg} = \sum_{t \in T} \gamma_t \tag{3.19}$$

where γ_t is the degradation cost in each time step, defined in Eq. (2.8) in Section 2.1.2.

Considering the equations given above, the objective function becomes:

$$\min_{\substack{\forall t \in T \\ \forall m \in M}} C_{tot}(t,m) = \sum_{t \in T}(c_{el,t} \cdot P_{grid,b,t}\Delta t - c_{feed-in,t} \cdot P_{grid,s,t}\Delta t + \gamma_t) + \sum_{m \in M}(c_{peak,m} \cdot P_{peak,m}) \quad (3.20)$$

3.3.3 Linear Programming

The objective function and most of the equations and constraints have linear relationships, making linear programming (LP) well suited to solve the optimization problem. It should be noted, however, that some of the equations and constraints have been simplified in order to obtain a model which can easily be solved to find the optimal solution. In reality, these models of real life scenarios may be much more complex, e.g. the battery degradation model as described in Section 2.1.1. Nevertheless, the simplifications can be justified as linear optimization provides unambiguous, repeatable results without requiring large computational efforts as compared to other optimization methods [12].

However, the battery degradation model still contains non-linear parts. Seeing as LP requires all equations and constraints to be linear, linearization needs to be applied. Referring to reference [1], the non-linear equations (3.14) and (3.15) are linearized as follows: Eq. (3.14) is transformed into (3.21) and (3.22), and Eq. (3.15) is transformed into (3.23) and (3.24).

$$DP_t \geq DP_{cyc,t} \quad (3.21)$$

$$DP_t \geq DP_{cal,t} \quad (3.22)$$

$$DP_{cyc,t} \geq 0.5 \cdot (\rho_t - \rho_{t-1}) \quad (3.23)$$

$$DP_{cyc,t} \geq 0.5 \cdot (-\rho_t + \rho_{t-1}) \quad (3.24)$$

However, there are still non-linearities in this model: when looking at Fig. 2.2 from Section 2.1.1.1, it becomes evident that there is a non-linear relationship between the DOD and the cycle life of the NMC battery. Seeing as the cyclic degradation, ρ_t, is defined as the inverse of the cycle life, Eq. (3.23) and (3.24) contain non-linear parts and need to be further linearized.

3.3.3.1 Piecewise Linearization using Special Order Sets

In order to model the non-linear relationship between the cyclic degradation and DOD, piecewise linearization is applied to the inverse of Fig. 2.2: the curve is divided into n linear segments, connected through $n+1$ points, as seen in Fig. 3.3. For a specific DOD value located between two points, the resulting degradation percentage is found based on the linear function of the segment connected by these two endpoints. In LP, this can be modelled by using special order sets of type 2 (SOS2). A SOS of type 2 is an ordered set of variables, where at most two variables can be non-zero for each time period. If two variables are non-zero, these must be adjacent. These sets are used in "branch and bound"[1] optimization methods to provide a more intelligent and efficient way of solving the problem. A linear model containing such sets becomes a discrete optimization model, even though the members of the set may themselves be continuous. As such, a mixed integer linear optimizer is required to solve the problem [33].

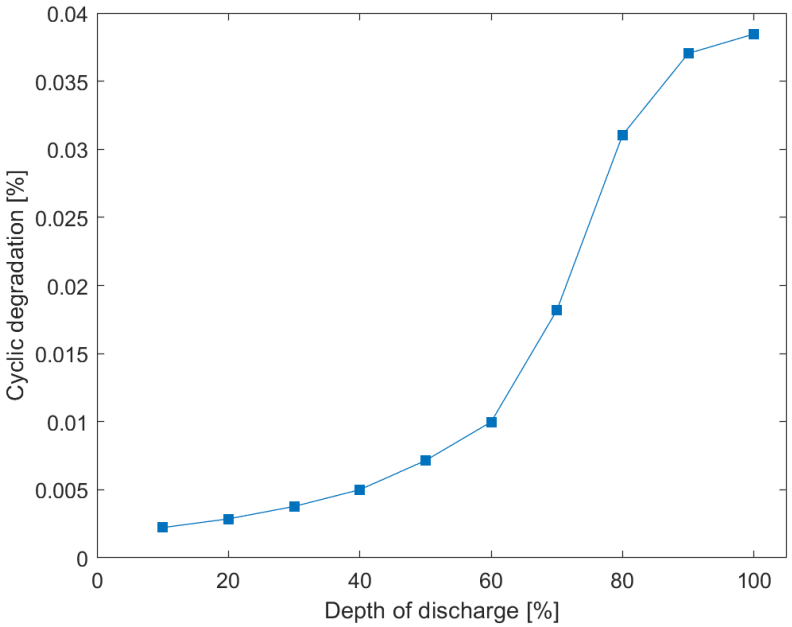

Figure 3.3: Piecewise linearization of the cyclic degradation versus DOD curve for a NMC battery

[1]The solution method forms a rooted tree, where the root is the initial problem formulation. When optimizing, branches are formed from the root, and each branch is a subset of the solution set. Each branch, with its distinct solution, is checked against constraints and discarded if these are not met or if it cannot produce a better solution than the best one found so far. More on this optimization method can be found in [33].

The piecewise linearization using SOS2 is shown in equations (3.25) through (3.27), where index i indicates point i on the piecewise linear curve. Here, $deg_{t,i}$ represents the degradation, $dod_{t,i}$ the depth of discharge, and $w_{t,i}$ the SOS2 variable of point i.

$$\rho_t = \sum_{i \in I} deg_{t,i} \cdot w_{t,i} \tag{3.25}$$

$$DOD_t = \sum_{i \in I} dod_{t,i} \cdot w_{t,i} \tag{3.26}$$

$$\sum_{i \in I} w_{t,i} = 1 \tag{3.27}$$

The SOS2 property of having at most two non-zero variables which have to be adjacent, ensures that we are always on the piecewise linear function. This could also have been modelled using binary variables, however special ordered sets are usually preferred as they may provide significantly computational savings [33].

3.3.4 Model Formulation

The model formulation, including the objective function as well as all equations and constraints, is shown below.

$$\min_{\substack{\forall t\in T\\ \forall m\in M}} \quad \sum_{t\in T}(c_{el,t}\cdot P_{grid,b,t}\Delta t - c_{feed-in,t}\cdot P_{grid,s,t}\Delta t + \gamma_t) + \sum_{m\in M}(c_{peak,m}\cdot P_{peak,m})$$

$$\begin{aligned}
\text{s.t.} \quad P_{pv,t} + P_{grid,b,t} + \eta_{inv}P_{disch,t} - P_{grid,s,t} - \tfrac{1}{\eta_{inv}}P_{charge,t} - P_{load,t} &= 0 && \forall t\in T\\
E_{bat,t} - E_{bat,t-1} - \eta_{charge}P_{charge,t}\Delta t + \tfrac{1}{\eta_{disch}}P_{disch,t}\Delta t &= 0 && \forall t\in T\\
SOC_t - \tfrac{E_{bat,t}}{E_{bat}^{nom}\cdot SOH_t} &= 0 && \forall t\in T\\
DOD_t + SOC_t &= 1 && \forall t\in T\\
SOH_t - SOH_{t-1} + 0.2DP_t &= 0 && \forall t\in T\\
DP_{cal,t} - \tfrac{100\%}{L_{cal}} &= 0 && \forall t\in T\\
\rho_t - \sum_{i\in I} deg_{t,i}\cdot w_{t,i} &= 0 && \forall t\in T\\
DOD_t - \sum_{i\in I} dod_{t,i}\cdot w_{t,i} &= 0 && \forall t\in T\\
\sum_{i\in I} w_{t,i} &= 1 && \forall t\in T\\
P_{grid,b,t} &\le P_{grid}^{max} && \forall t\in T\\
P_{charge,t} &\le \eta_{inv}P_{inv}^{nom} && \forall t\in T\\
P_{disch,t} &\le P_{inv}^{nom} && \forall t\in T\\
E_{bat,t} &\le E_{bat}^{nom}\cdot SOH_t\cdot SOC_{max} && \forall t\in T\\
SOC_t &\le SOC_{max} && \forall t\in T\\
SOC_t &\ge SOC_{min} && \forall t\in T\\
DP_t &\ge DP_{cyc,t} && \forall t\in T\\
DP_t &\ge DP_{cal,t} && \forall t\in T\\
DP_{cyc,t} &\ge 0.5\cdot(\rho_t - \rho_{t-1}) && \forall t\in T\\
DP_{cyc,t} &\ge 0.5\cdot(-\rho_t + \rho_{t-1}) && \forall t\in T\\
E_{bat,t} &\ge E_{bat}^{nom}\cdot SOH_t\cdot SOC_{min} && \forall t\in T\\
P_{peak,m} &\ge P_{grid,b,t} && \forall t,m\in M\\
P_{grid,b,t}, P_{grid,s,t}, P_{charge,t}, P_{disch,t} &\ge 0 && \forall t\in T
\end{aligned}$$

4 | Holmen Swimming Facility

The system under study is Holmen swimming facility, located in Asker, Norway and opened in mid-2017. With 45% annual energy savings[1] and a PV system covering around 12% of the annual electricity demand, it is considered a passive house and is one of the countries most energy efficient swimming facilities [34]. However, their power peaks are high, meaning their total cost of electricity may be substantial even with the annual energy savings. Implementing a BESS can shave these peaks, and may prove economically beneficial if the savings from peak shaving operations are higher than the operational cost of the battery.

All data on load demand and solar production was collected using Gurusoft®, with access provided by Holmen swimming facility and Asker municipality. Here, Sections 4.1 and 4.2 give a brief introduction to the loads and PV systems, respectively, while more details on the specific data is presented in Chapter 5. Section 4.3 presents the cost of electricity for the facility.

4.1 The Loads

The electrical loads of the system consist of all units requiring electrical power, which can be provided by either the grid or by the PV systems. The electrical loads of the swimming facility are listed below, from the most to the least demanding as given in Gurusoft®:

- Saunas and ventilation
- Electric boiler
- Swimming pools

[1] Compared to swimming facilities built according to today's regulations

- Heat pump
- Lighting
- Energy plant and heaters
- Charging of electric vehicles
- Reserve

4.2 The PV System

Holmen swimming facility has installed several PV systems on both the rooftop and facades, using Solel. Table 4.1 gives an overview of the characteristics of each one, based on information provided by the installer [35].

Table 4.1: PV system characteristics of Holmen swimming facility

Location	Size	Tilt angle	Solar angle	PR[a]
Rooftop	53,5 kWp	10°	160°(S/SE)	80%
Facade	31,32 kWp	90°	160°(S/SE)	85%
Bike rack	4,32 kWp	10°	160°(S/SE)	85%

[a]The performance ratio (PR) is the relationship between actual and theoretical energy output, and is less than 100% due to system losses such as shading and heating.

4.3 The Cost of Electricity

As shown in Eq. (2.10) in Section 2.3.1, the total cost of electricity consists of three parts: the cost of purchasing power from the grid, the revenue from selling power to the grid (if any), and the cost of the highest peak power demand each month. These cost are based on tariffs set by the local network company, which for Asker is Hafslund Net.

The cost of purchasing power from the grid depends on the energy tariff, set to be a seasonal dependant flat rate by Hafslund Net. However, a time dependent rate is assumed in this study to reflect the near future trends, as presented in Section 2.3. More specifically, a RTP scheme is chosen, based on the Elspot day-ahead prices for Oslo in 2017, collected from Nord Pool [6]. The spot prices for

two arbitrary winter and summer months are shown in Fig. 4.1, where it can be seen how the prices are higher during the winter with an average price of 0.28 NOK per kWh, compared to 0.22 NOK per kWh in the summer. It can also be seen that the prices fluctuate more during the summer month, which may be due to a higher penetration of renewable energy.

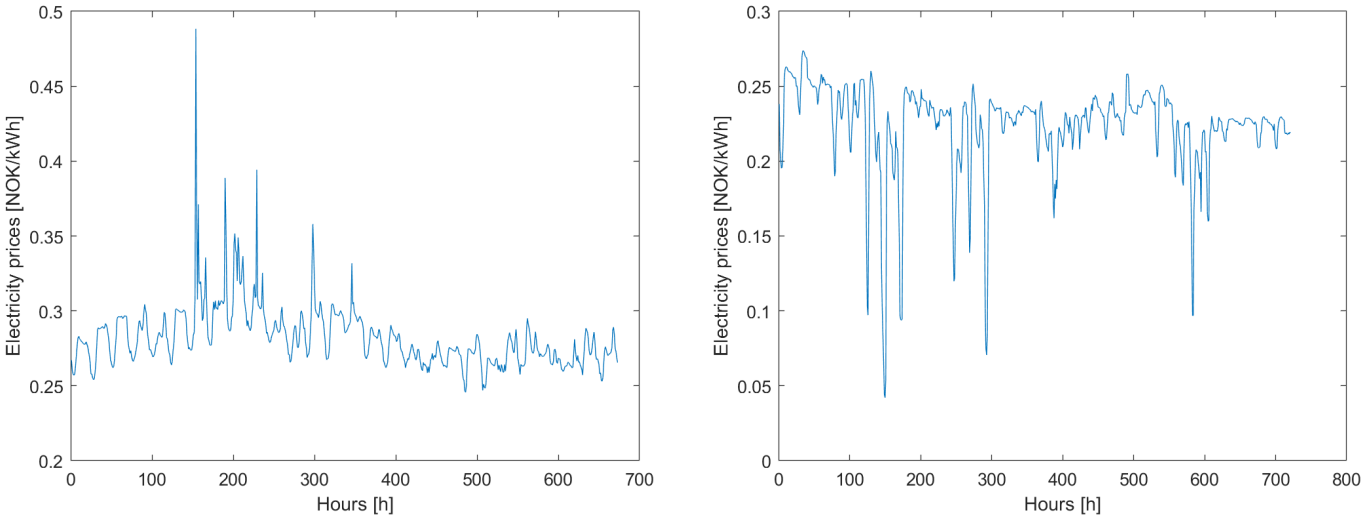

(a) February **(b)** June

Figure 4.1: Spot prices for Oslo (2017), based on data from [6]

A revenue from selling power to the grid may be generated if the solar production exceeds the load demand. The revenue is based on a feed-in tariff, which in turn is based on a deal the customer makes with its local power supplier. For this study, a constant value of 0.04 NOK per kWh is chosen based on the feed-in tariff provided by Agder Energy [36].

The cost of peak demand is subject to the charges presented in Table 4.2 as of 2018, based on data from Hafslund Net [7].

Table 4.2: Peak demand tariffs, based on data from Hafslund Net [7]

	Demand tariffs
Winter 1 (Jan, Feb, Dec)	150 NOK/kWp/month
Winter 2 (Mar, Nov)	77 NOK/kWp/month
Summer (Apr-Oct)	11 NOK/kWp/month

5 | Solution Method

This chapter gives a brief explanation on how the model presented in Section 3.3.4 is implemented using available commercial software, and how important system parameters are decided. The model is written in The General Algebraic Modeling System (GAMS) and solved using Gurobi. All large parameter data is read from Excel, and loaded to GAMS using functions in Matlab. The results obtained from running the optimization in GAMS are read back to Matlab and further manipulated, in order to make the results presentable in the form of plots and graphs.

In order to capture the seasonal characteristics with regards to PV generation and load demand, a planning horizon of one year with hourly time increments is considered in the simulations. A time resolution of one hour was chosen based on the energy market operating on an hourly basis, and is a compromise between obtaining accurate results and lowering the computational speed. As such, the one-year simulation covers a total of 8760 time intervals.

Here, Section 5.1 gives an overview of the characteristics of the chosen optimization software, and Section 5.2 describes how important system parameters are estimated.

5.1 Modelling in GAMS

GAMS is a high-level modeling system for mathematical programming and optimization, specifically designed for modelling linear, non-linear and mixed integer optimization problems [37]. As opposed to languages using a matrix data structure where all equations and constraints need to be translated into matrices, like Matlab, GAMS uses an algebraic modeling language. This implies that the optimization model is a collection of algebraic equation, and closely resembles the mathematical model formulation of Chapter 3. Other advantages of using GAMS are listen below, based on reference [38].

- Due to the equation based modelling language, building large, complex models is easy, and the models can quickly be adapted to new situations.
- The model formulation is independent of the model data, allowing you to run the model for different data sets without changing the model formulation.
- It comes with several state-of-the-art sovlers, and the model formulation is independent of the chosen solver: after formulating the equations, you simply tell GAMS which solver you want to use and what type of problem you have (linear, non-linear etc.), meaning you can try different solvers without changing the model formulation.
- The resulting solution report is easy to read, and you can choose which variables you want to display. Moreover, the output can easily be transferred to other programs, like Matlab or Excel, to represent the solution in a graphical way.

5.2 Estimating Important System Parameters

As previously mentioned, Holmen swimming facility was opened in mid-2017. However, due to initial problems with installing measurement tools, no recorded data on load demand or solar production is available before January 2018. Thus, in order to be able to analyze the system behaviour over one full year, estimates on future demand and production have been made. Moreover, both the initial battery size and the maximum power that can be drawn from the grid are parameters, hence they need to be set prior to solving. Seeing as their chosen values may have a potential large impact on the solution results, it is desirable to find close to optimal values before solving. The following sections describe the estimation approaches used.

5.2.1 Estimating Yearly Load Demand

The yearly load demand was estimated based on historical data from January to April 2018, and the following assumptions were made:

- The load data for similar months was "mirrored" using actual load data, i.e. the load demand for 31^{st} of December was assumed equal to the demand for 1^{st} of January, the load demand for 30^{th} of December was set equal to the demand for 2^{nd} of January, and so on. This was done for September to December as only data from January to April was available.

- The load demand for May was assumed equal to the load demand for April.
- The load demand for the first two weeks of June was assumed equal to the two last weeks of May.
- The load demand for the second two weeks of June was assumed equal to the two first weeks, reduced by 20% to reflect the start of the school's summer holiday.
- The load demand for July was assumed equal to the load demand for June without reduction, reduced by 40% to reflect the affects of the public holiday.
- The load demand for August was assumed equal to the "mirrored" load demand of June.

The assumptions described above are based on load demand trends for other swimming facilities in Norway [39], however the real load demand will vary from the estimations. This should be kept in mind when analyzing the simulation results.

The yearly load profile with both historical and estimated data is shown in Fig. 5.1a, with a total annual consumption of around 2,306 MWh. As seen from the figure, the load demand is higher during the winter months and at its lowest in July due to the assumptions made on load estimations. Moreover, high peaks can be observed for all months when looking at Fig. 5.1b. Seeing as the peak demand tariff is high, especially for the winter months as shown in Table 4.2 from Section 4.3, peak shaving may provide significant savings on the demand charge for the customer. It should be noted that the peak power demands from Fig. 5.1b are the net peak demands after the solar production has been subtracted from the load demand. The data on solar production is discussed in the following section.

5.2.2 Estimating Solar Production

By using the data given in Table 4.1 from Section 4.3, the expected hourly solar production was calculated for each individual system using PVWatts® Calculator. PVWatts® is an online product from the National Renewable Energy Laboratory (NREL) that calculates annual production from PV systems at any given location. To estimate production, it uses typical year weather data[1] which

[1]Each month is selected from a different year, giving a more representative and long-term data than data collected from a given year.

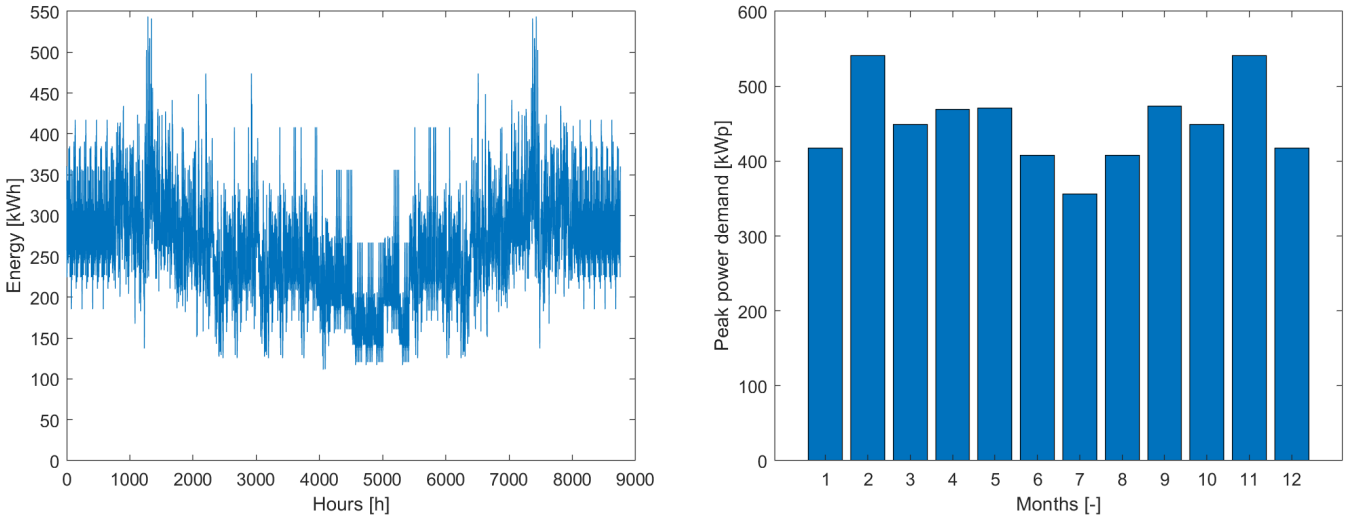

(a) Yearly load demand

(b) Net peak power demand

Figure 5.1: Estimated load demand for Holmen swimming facility

represents the long-term solar resource at a location and thus produces accurate estimates [40]. Although Asker was not available as a location, data from Fornebu in Oslo was used as they lie at approximately the same latitude and longitude.

The total annual solar production was calculated to be 62.4 MWh. Fig. 5.2a and 5.2b show the solar production for each PV system for two arbitrary winter and summer weeks, respectively. The chosen weeks are week 8 (mid-February) and week 24 (mid-June). As seen from the figures, the solar production is higher during summer due to more irradiation. Moreover, since the irradiation data is based on historical data, daily changes in weather are accounted for. This is especially evident when looking at Fig. 5.2a, where the solar production is significantly lower for the two last days of the week, most likely due to clouds or shading from snow.

Fig. 5.3 shows the load demand and total solar production in the same plot for week 8 and week 24. As seen from the figure, the load demand is considerably higher than the solar production, even in the summer.

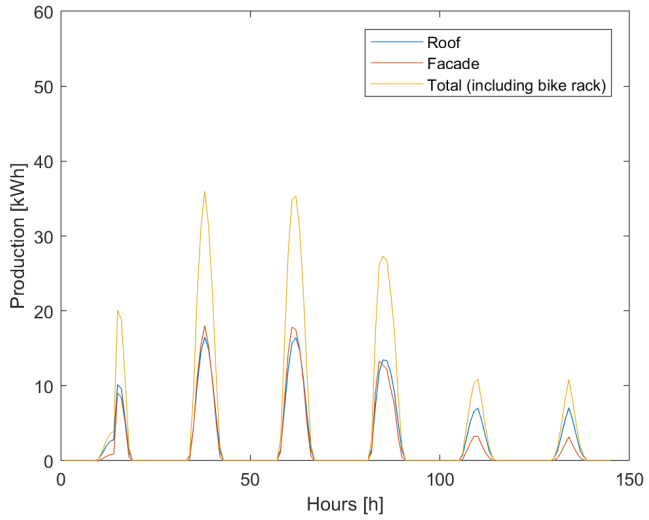

(a) Weekly solar production, week 8

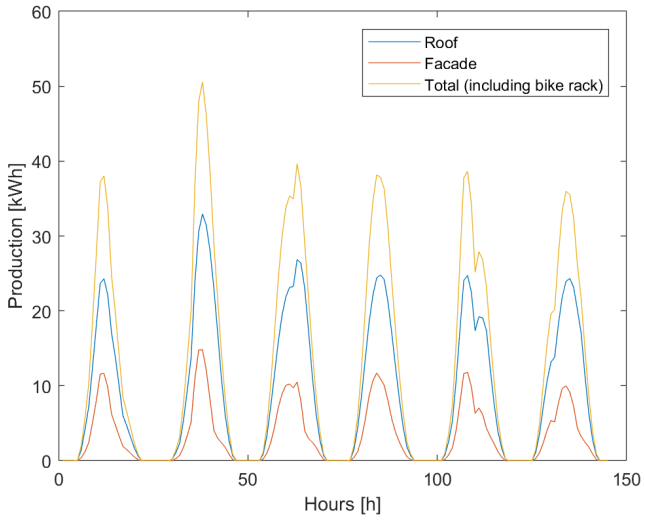

(b) Weekly solar production, week 24

Figure 5.2: Weekly solar production for two arbitrary winter and summer weeks

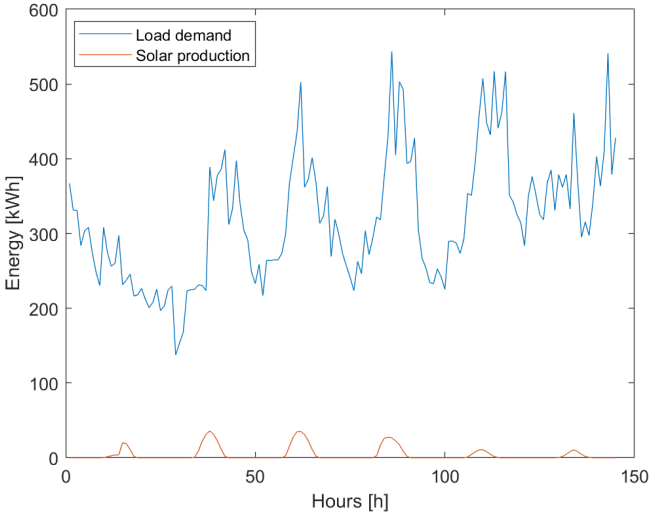

(a) Weekly load demand and solar production, week 8

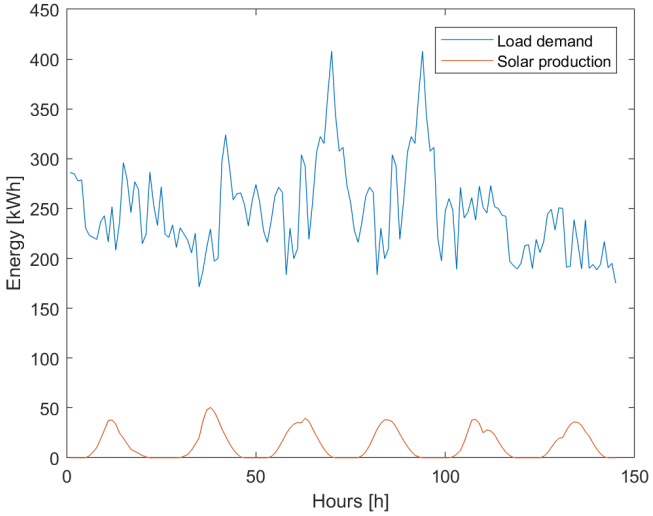

(b) Weekly load demand and solar production, week 24

Figure 5.3: Weekly load demand and solar production for two arbitrary winter and summer weeks

If the solar production never exceeds the load demand, there will be no excess power to charge a potential battery. As such, inclusion of a BESS may not be economically profitable as it would have to be charged from the grid, thus increasing the cost of energy. However, if the difference between the off-peak and on-peak electricity prices are high, the battery may generate revenue as it can charge from the grid during off-peak hours and discharge when prices are high. Moreover, using the battery for peak shaving purposes may reduce the cost of peak power substantially.

5.2.3 Estimating E_{bat}^{nom} and P_{grid}^{max}

Both the nominal battery capacity, E_{bat}^{nom}, and the maximum amount of power that can be drawn from the grid, P_{grid}^{max}, are parameters in the simulation model, meaning they are set prior to solving. Seeing as the cost of the battery and the peak demand charge are highly dependent on E_{bat}^{nom} and P_{grid}^{max}, respectively, the chosen values will largely affect the simulation results. As such, it is important to decide on the optimal parameter values before solving in order to minimize the objective function, i.e. the total system cost.

In order to find the optimal parameter values, simulations of the proposed system were carried out with a one month time horizon for different values of E_{bat}^{nom}. The simulations returned both the optimal value of P_{grid}^{max} and the resulting system cost. A one month time horizon was chosen as it significantly reduces the simulation time when compared to one year, while still being able to include the peak demand charge. The peak power demand for the system without BESS is shown in Fig. 5.1b, where the highest peaks occur in February and November. Seeing as February has the highest demand tariff of the two (150 versus 77 NOK/kWp/month), it was chosen as the test month in order to capture the most extreme scenario. The resulting system cost as a function of E_{bat}^{nom} is shown in Fig. 5.4.

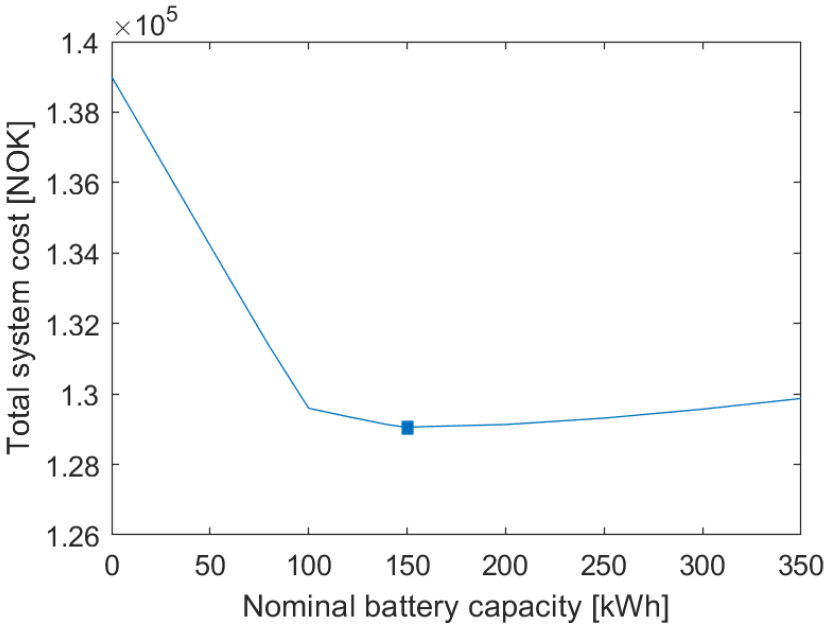

Figure 5.4: Optimal system cost as a function of battery capacity for February

As can be seen from the figure, the optimal battery capacity is found to be 150 kWh, which in turn sets the optimal value of P_{grid}^{max} to be 455,38 kWp. It can also be observed that increasing the battery size beyond the optimal value has little effect on the total system cost. A larger battery will be able to provide more peak shaving while also being more expensive, causing only slight changes in the total system cost. However, as long as the battery is large enough to provide sufficient peak shaving, the smaller battery is preferred: the battery pack takes up less space, is lighter in weight and the initial investment costs are lower.

6 | Case Study Results

In this chapter, results obtained from simulating the multi integer LP (MILP) optimization problem in GAMS are presented. The simulations are carried out on the proposed system shown in Fig. 3.1, referred to as the base case (BC), with the equations and constraints as described in Chapter 3. All parameter values relevant for the system, as well as those used in the simulation model, are shown in Table 6.1. A one year system simulation of the BC, with a total of 8760 time steps, took approximately one hour on a computer with 64-bit Windows 10 Enterprise, Intel® Core™ i7-6650U 2.20 GHz CPU and 16 GB of RAM.

Table 6.1: Parameter values used for the BC

(a) System parameters

Parameter	Value
$P_{load,t}$	Input data
$P_{pv,t}$	Input data
$c_{el,t}$	Day-ahead prices, Oslo (2017)
$c_{feed\text{-}in,t}$	0.04 NOK/kWh
$c_{peak,m}$	See Table 4.2
P_{inv}^{nom}	150 kW
E_{bat}^{nom}	150 kWh
η_{inv}	98%
η_{rt}	96%
SOC_{min}	10%
SOC_{max}	90%
L_{cal}	15 years
c_{bat}	3,600 NOK/kWh[a]

[a]Based on central estimates on the cost of NMC BESS for 2016 (Fig. 2.4 from Section 2.1.2)

(b) Simulation parameters

Parameter	Value
T	8760
M	12
Δt	1 h
P_{grid}^{max}	455.38 kW
E_{bat}^{init}	0 kWh
SOH_{init}	100%

Several sensitivity analyses on important system parameters are also investigated for the BC alternative. This includes sensitivity on the cost of the battery, i.e. the BESS, as well as the energy and peak demand tariffs. Lastly, a 2030 scenario is simulated in order to analyze the impacts of implementing the proposed system in the future.

Several simplifications and assumptions have been made prior to solving the optimization problem, which should be kept in mind when viewing and analyzing the results. Although presented throughout the paper, they are summarized below for convenience:

- The load demand and solar production are estimated based on historical data, as described in Section 5.2.
- The hourly load demand and solar production are known prior to solving the problem, i.e. a perfect forecast model is assumed.
- The battery is based on the characteristics of a lithium-ion NMC battery.
- The C-rate of the battery is assumed equal to one, meaning the battery can charge or discharge all available energy in one hour within the limits of the BESS inverter.
- Both the efficiency of the BESS inverter and the round-trip efficiency of the battery are considered constant.
- A RTP scheme is assumed, and the hourly energy tariffs are set equal to the Elspot day-ahead prices in Oslo for 2017.
- The cost of the BESS is assumed to include all component cost and cost of installation, and is set equal to the central cost estimates for NMC technologies from 2016, as seen in Fig. 2.4.
- The degradation cost of the battery is modelled as a percentage of the initial investment cost, such that when the battery reaches the end of its lifetime the initial costs are accounted for. All other operational costs, such as the cost of maintenance, are neglected.

6.1 The Present Alternative

The present alternative, i.e. the system without a BESS, is shown in Table 6.2, calculated based on the energy and peak power tariffs from Table 6.1. When analyzing the results from the model simulations, these costs are used as a basis for interpreting whether the system under study is economically beneficial. As seen from the table, the cost of peak power contributes to 34% of the total cost of electricity, which is a substantial amount.

Table 6.2: The present alternative

Grid only	
Energy drawn from the grid (net load)	2,243,653 kWh
Total cost of energy	612,767 NOK
Total cost of peak power	315,952 NOK
Total cost of electricity	928,719 NOK

6.2 The Base Case (BC)

The yearly operation of the proposed system was optimized using the parameters given in Table 6.1, and the simulation results are shown below. It should be noted that for the rest of this chapter, the battery power is considered positive when charging (as seen from the battery). Fig. 6.1a shows the system operation in terms of hourly power flow to and from the different components. The net load is the solar production subtracted from the load demand. The power flowing to and from the battery is further highlighted in Fig. 6.1b. Fig. 6.1c and 6.1d show the degradation and the state of health of the battery, respectively. More detailed figures of the system operation for an arbitrary week are presented in Section 6.2.1.

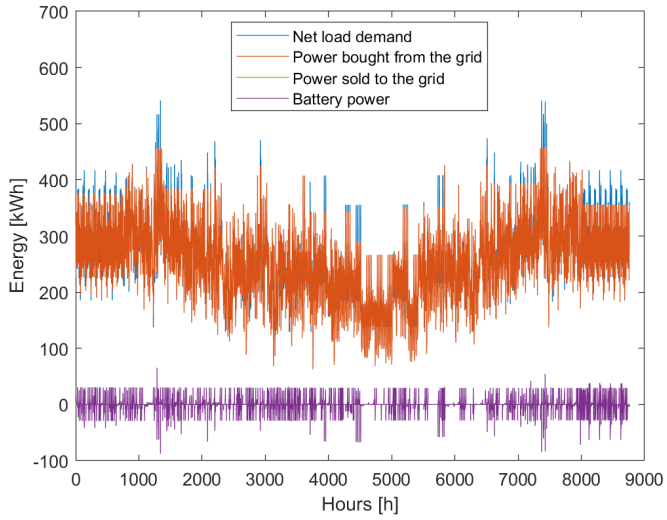

(a) System operation

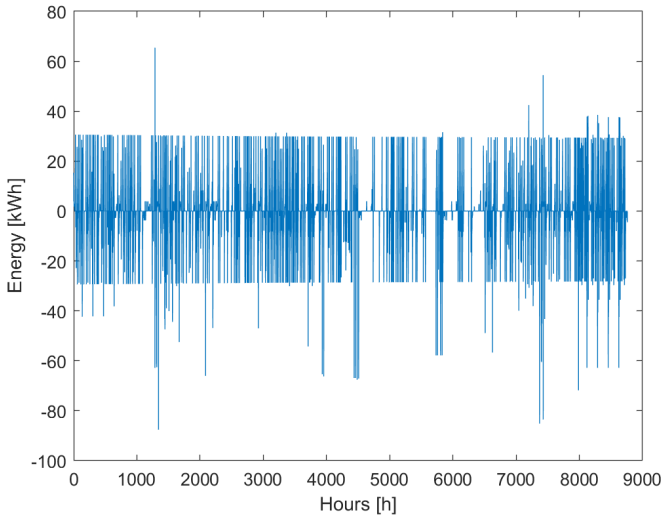

(b) Power to and from the battery

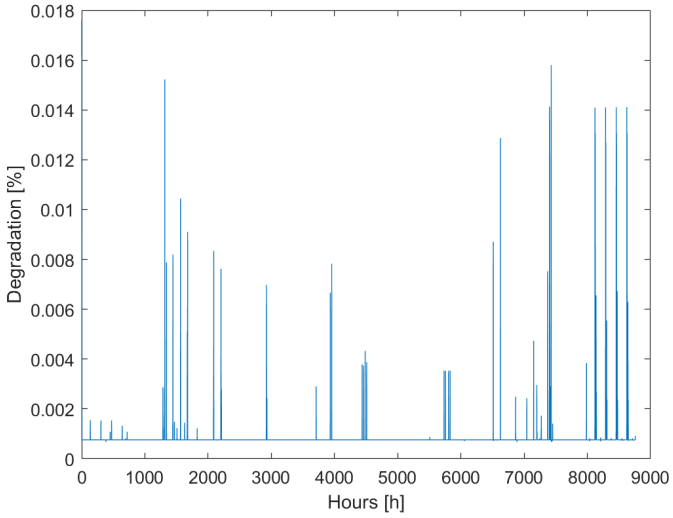

(c) Battery degradation

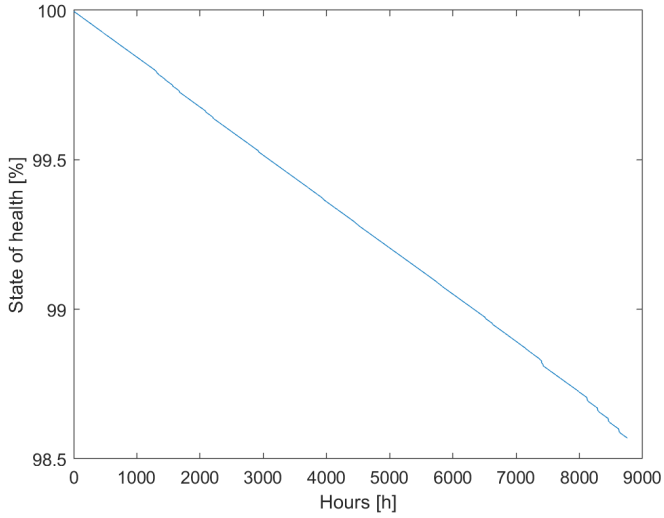

(d) Battery state of health

Figure 6.1: BC results for one year

As can be seen from Fig. 6.1a, the net load is always positive and thus the battery is effectively charged from the grid. Moreover, the power sold to the grid is equal to zero throughout the year as it is more profitable to supply the loads with solar power than to sell that power back to the grid. The operation of the battery is highlighted in Fig. 6.1b, where it can be seen how the battery supplies the load with large amounts of power during hours of high peak demand to perform peak shaving.

However, peak shaving comes at a price: charging and discharging the battery with large amounts

of power causes the battery to degrade faster, as seen in Fig. 6.1c, which in turn results in high operational costs. In fact, the highest cost of degradation in one hour is found to be 85.3 NOK. In order for peak shaving to be economically attractive, the operational cost of the battery (the cost of degradation plus the cost of charging the battery, including losses) has to be less than the revenue gained from shaving the peak in that hour. After one year of operation, the SOH of the battery is reduced to 98.57% as seen from Fig. 6.1d.

The effect of peak shaving is further analyzed in Fig. 6.2, where Fig. 6.2a shows the monthly peak power demand with and without BESS, and Fig. 6.2b shows the amount of peak power shaved for each month. The highest amount of peak shaved, 85.6 kW, occurs in February, having both the highest initial peak load demand and the highest peak demand charge. The savings from performing peak shaving on the highest peak in February amounts to 12,874 NOK, which is substantially higher than the corresponding operational cost of 64.7 NOK. The calculations are shown in Appendix A.

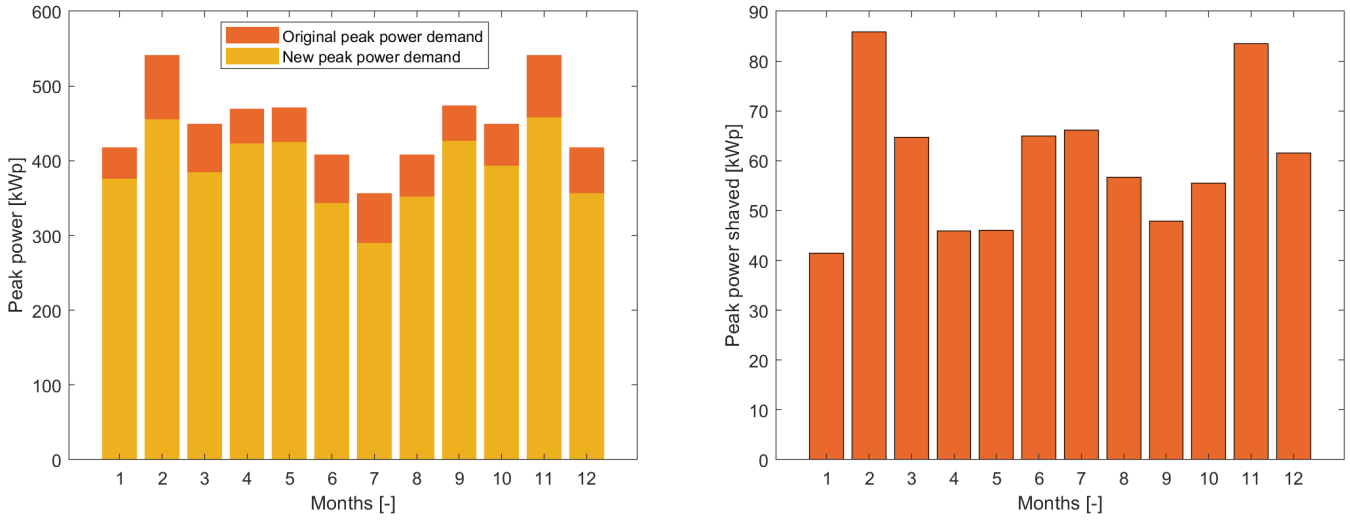

(a) Monthly peak power: with and without BESS

(b) Monthly peak shaving with BESS

Figure 6.2: BC results for one year: peak shaving

A summary of the most important results are listed in Table 6.3, and analyzed below.

Table 6.3: Results from the BC

Results: BC	
Energy drawn from the grid	2,245,284 kWh
Compared to original system	*+ 1,631 kWh*
Total degradation	7.15%
Total cost of degradation	38,636 NOK
Compared to original system	*+ 38,636 NOK*
Total cost of energy	612,112 kWh
Compared to original system	*- 655 NOK*
Total cost of peak power	271,998 NOK
Compared to original system	*- 43,954 NOK*
Total system cost (objective function)	922,747 NOK
Compared to original system	*- 5,972 NOK*

- During one year of operation, the battery degrades by 7.15%, leading to a 1.43% reduction in the SOH. Assuming no changes in the system characteristics, the battery can thus operate another 14 years before reaching the end of its lifetime.
- There is a higher amount of energy drawn from the grid than for the original system, however, the total cost of energy is reduced by 0.1%. This is likely due to the battery being able to exploit volatile price signals: it may charge from the grid when the price of electricity is low, and discharge when the price is high.
- The total cost of peak power is reduced by 13.9% due to the battery being used for peak shaving, and the savings from peak shaving alone exceeds the total cost of degradation. The cost of peak power now contributes to 30.7% of the total cost of electricity, a reduction from the original system.
- By implementing a BESS, the yearly system costs are reduced by 5,972 NOK (0.64%).

6.2.1 BC: an Arbitrary Week

In order to be able to study the system operation and battery degradation in more detail, the results from an arbitrary week are shown in Fig. 6.3. Week 8 was chosen as it has both large variations in net load demand and high power peaks. The same results for an arbitrary summer week (week 24) are shown in Appendix B, however they are not further discussed.

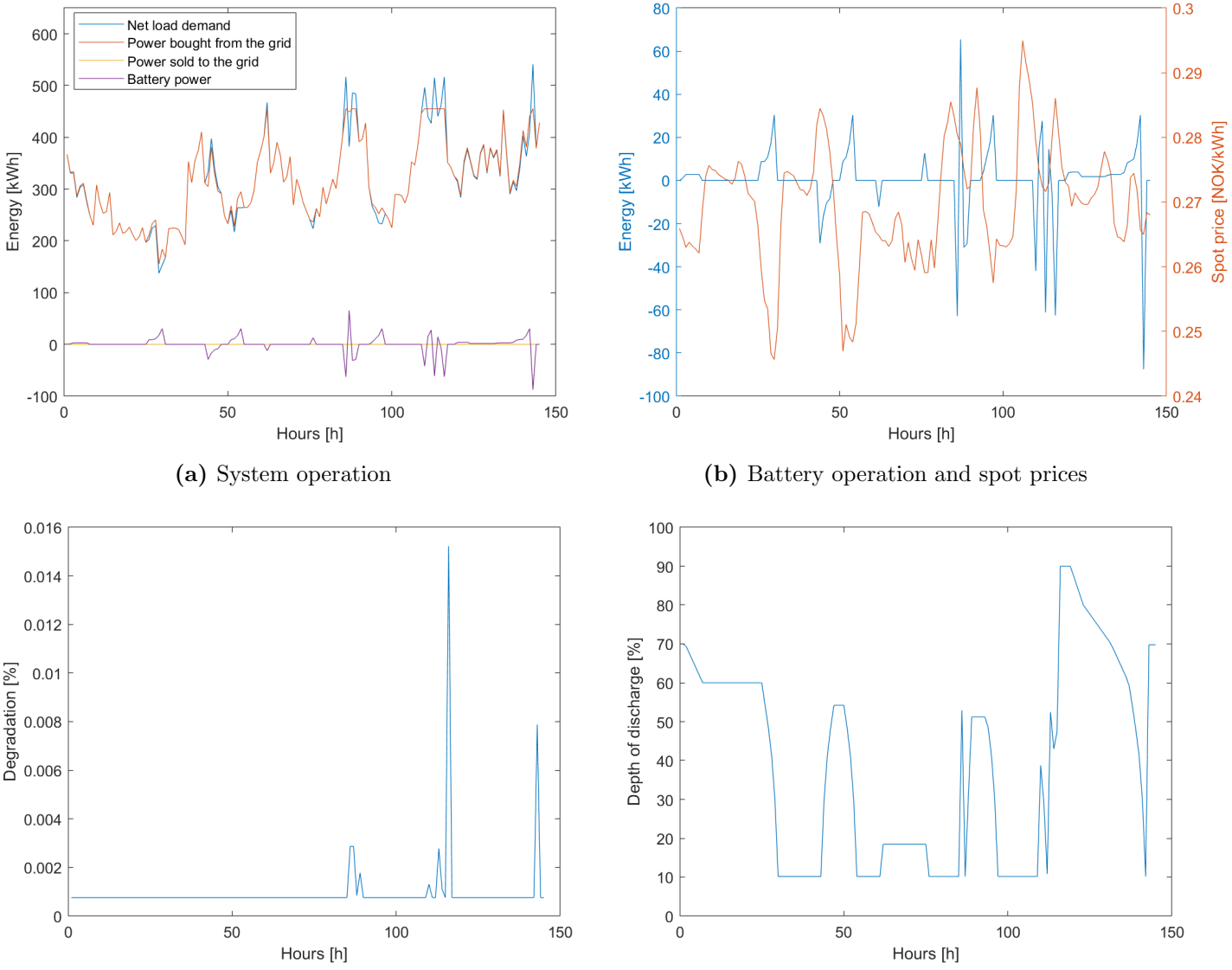

(a) System operation

(b) Battery operation and spot prices

(c) Battery degradation

(d) Battery depth of discharge

Figure 6.3: BC results for week 8

By studying the figures above, several interesting facts can be observed:

- As suspected, the battery is used for price arbitrage operation when subject to a RTP scheme, as seen in Fig. 6.3b: the battery charges during hours of low spot prices, and discharges when the spot prices are higher.
- During hours of high peaks, the battery is operated regardless of the spot price. For example, it can be seen that for around hour 90 the battery is charged even though the price of electricity is high, in order to discharge the following hour to shave the peak.
- Fig. 6.3c shows that the degradation is mostly constant and equal to the cyclic degradation, even when the battery is operating. As seen, the battery chooses to charge or discharge only small amounts whenever possible to exploit the volatile prices, while keeping the cost of degradation low. Moreover, this ensures that the battery can load up on energy and discharge during hours of high peaks.
- The correlation between the degradation percentage and the DOD becomes evident when comparing Fig. 6.3c and 6.3d: for deeper discharge levels, the degradation percentage is high. This is especially true for around hour 120, where the battery is discharged from a DOD level of 45% to the maximum level of 90%, causing a degradation of 0.015% and a cost of degradation of 82 NOK. Around hour 145 however, the degradation percentage is much lower even though the net change in DOD is higher (from 10% to 70%).

6.3 Sensitivity Analyses

In order to investigate how different parameters affect the optimal solution, sensitivity analyses are carried out on three important system parameters: the cost of the battery, the peak demand tariff and the energy tariff. Seeing as one simulation of the BC took around one hour, all sensitivity analyses have been carried out using a one month time horizon in order to save simulation time. More specifically, February was chosen as the simulation month due to the characteristics described in Section 5.2.3. It should be kept in mind that the simulation results obtained for one month will differ from those obtained for a year, however they can be useful for noting trends when varying the parameters.

6.3.1 Sensitivity on the Cost of the Battery (SA1)

As discussed in Section 2.1.2, the cost of battery storage systems are rapidly decreasing, expected to be halved by 2030. As such, it is important to see how reductions in these costs will affect the optimal results. In the following analysis, the simulations have been carried out for different nominal battery capacities while gradually decreasing the cost of the battery, c_{bat}, from its initial value to a 50% decrease. The results are shown in Fig. 6.4. It should be noted that only battery capacities from 100 to 500 kWh have been studied.

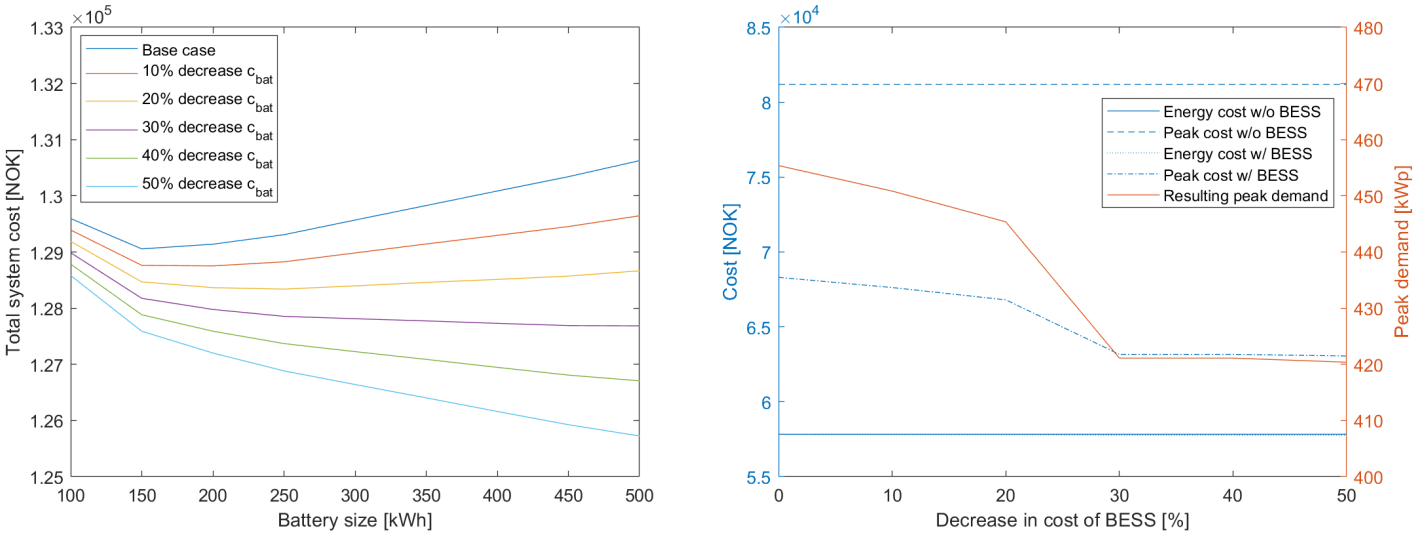

(a) System cost as a function of E_{bat}^{nom} for different c_{bat}

(b) System costs as a function of cost decrease

Figure 6.4: Sensitivity on the cost of the battery (SA1)

As seen from Fig. 6.4a, the overall trend is for a decrease in the total system cost with decreasing cost of the battery, however the savings depend on the size of the battery: when decreasing c_{bat} by 50%, the system costs decrease 1% for a 150 kWh battery and 3.8% for a 500 kWh battery compared to the BC. It can also be seen that different cost scenarios lead to different optimal storage capacities: a decrease in the cost of the battery leads to an increase in the optimal battery size. However, this has little effect on the system cost: for a 50% increase in c_{bat}, the total system cost is reduced by only 0.14% when increasing E_{bat}^{nom} from 150 to 490 kWh.

Fig. 6.4b shows the energy and peak demand costs of the system with and without BESS as a function of the percentage decrease in c_{bat}. Moreover, the resulting peak demand for the system with

BESS is plotted. It should be noted that the system costs with BESS are found when simulating the system with the optimal battery capacities found from Fig. 6.4a. When looking at the figure, several observations can be made:

- The energy costs with and without BESS are approximately similar, even though the battery is charged by the grid. This was also shown for the BC, and is due to the battery being able to exploit the hourly variations in the energy tariff.
- There is a correlation between the cost of peak power and the resulting peak demand for the system with BESS, as can be expected. Moreover, it can be seen that the cost of peak power decreases with decreasing c_{bat}, which is related to the corresponding increase in the optimal size of the battery: with increasing capacity, the battery is able to shave a larger amount of peak power, thus reducing the peak power costs.
- The decrease in peak demand is high for a 20% to a 30% decrease in c_{bat}, due to the optimal battery size increasing drastically (from 240 to 490 kWh). It is however approximately constant between a 30% and a 50% decrease in c_{bat}. This can be explained by noting that these cases were simulated using almost the same optimal battery capacity (490-500 kWh), as the sensitivity analyses are only studied for battery sizes up to this value.
- For a 50% decrease in c_{bat}, the cost of peak power is reduced by 22% by implementing a BESS compared to the original system.

6.3.2 Sensitivity on the Peak Demand Tariff (SA2)

Due to the vast implementation of power-demanding devices like electric vehicles, there is an increased pressure on the grid to deliver high amounts of power. If these power peaks start approaching the capacity limit of the grid, the grid will need to be expanded. Seeing as grid expansion is extremely costly, alternative measures in terms of reducing the power peaks is preferable. For commercial customers who are already billed for their peak demand, a way of reducing their peaks could be to increase the peak demand tariff. This would encourage the customers to either shave their peaks or shift their load demand, thus relieving the grid of stress. In the following analysis, the simulations have been carried out for different nominal battery capacities while gradually increasing the peak demand tariff (c_{peak}) from its initial value to a 50% increase, to see how this affects the system costs. The results are shown in Fig. 6.5.

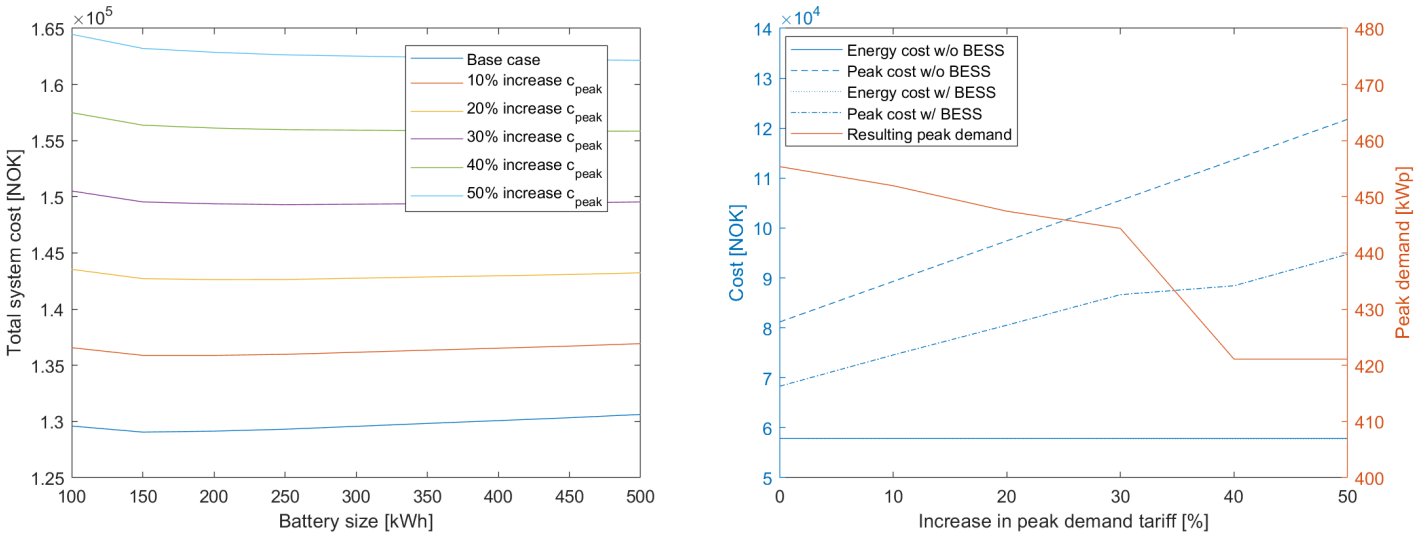

(a) System cost as a function of E_{bat}^{nom} for different c_{peak}

(b) System costs as a function of tariff increase

Figure 6.5: Sensitivity on the peak demand tariff (SA2)

As can be seen from Fig. 6.5a, the total system cost increase substantially when increasing the peak demand tariff: with a battery capacity of 150 kWh, the system cost increase by 5.3% when increasing c_{peak} only 10% - and by 26.4% when c_{peak} is increased by 50%. Moreover, as for SA1, increasing the nominal battery size over 150 kWh has little effect on the total system.

Fig. 6.5b shows the energy and peak demand costs of the system with and without BESS as a function of percentage increase in c_{peak}. As was the case for SA1, the energy cost with and without BESS are approximately similar. The following other observations can be made:

- The cost of peak demand increases when increasing the demand tariff, as can be expected. For a 50% increase in c_{peak}, the increase in peak demand costs are 38.7% and 50% for the system with and without BESS, respectively.
- While the peak cost increases linearly for the system without BESS, this is not the case for the system with BESS: between a 30% and 40% increase in c_{peak}, the slope is more gentle. This is due to the optimal battery capacity being drastically increased (from 240 to 490 kWh), thus decreasing the peak demand.
- As was the case for SA1, the peak demand is approximately constant between a 40% and a 50% increase in c_{peak} due to the two cases being simulated using the same optimal battery capacity of 500 kWh.

The total system cost as a function of percentage change in both C_{bat} and c_{peak} is shown in Fig. 6.6. When changing one parameter, the other is held constant. It should be noted that the problem is simulated for each case using the optimal battery size found from Fig. 6.4a and 6.5a.

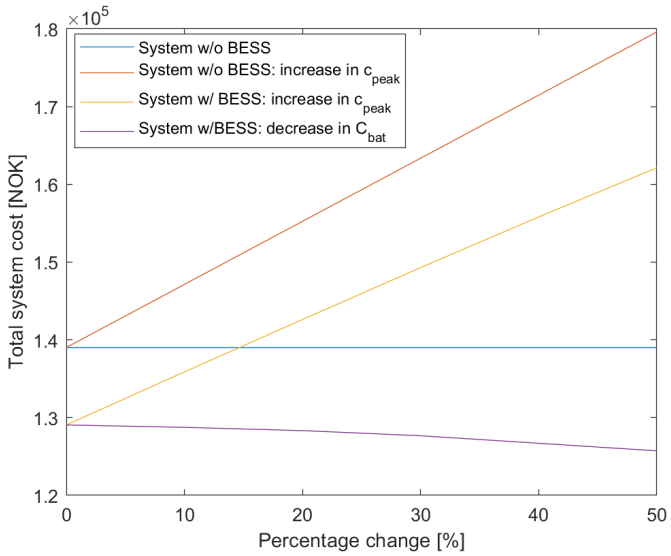

Figure 6.6: Total system cost as a function of percentage change for two system parameters

When studying the figure above, several observations can be made. Recall that the results are based on one month.

- The total system cost is strongly affected by an increase in the peak demand tariff, however the cost increase is higher for the system without BESS: for a 50% increase in c_{peak}, the system cost without BESS increases by 29.2%, compared to a 25.6% increase for the system with BESS.
- The total cost savings of installing a BESS for a 50% increase in the peak demand tariff is 17,476 NOK (9.7%).
- The total system cost is not as strongly affected by a decrease in the initial battery cost: when decreasing c_{bat} by 50%, the system cost with BESS decrease by 2.6%. The cost of the system without BESS is constant.
- The total cost savings of installing a BESS for a 50% decrease in the cost of the battery is 13,292 NOK (9.6%).

6.3.3 Sensitivity on the Energy Tariff (SA3)

Seeing as the spot prices in the Norwegian market are expected to become more volatile with higher price peaks in the future, as discussed in Section 2.3, it is important to see how this would affect the system operation. The Elspot day-ahead prices for February in 2017 for three different Nordic markets are shown in Fig. 6.7.

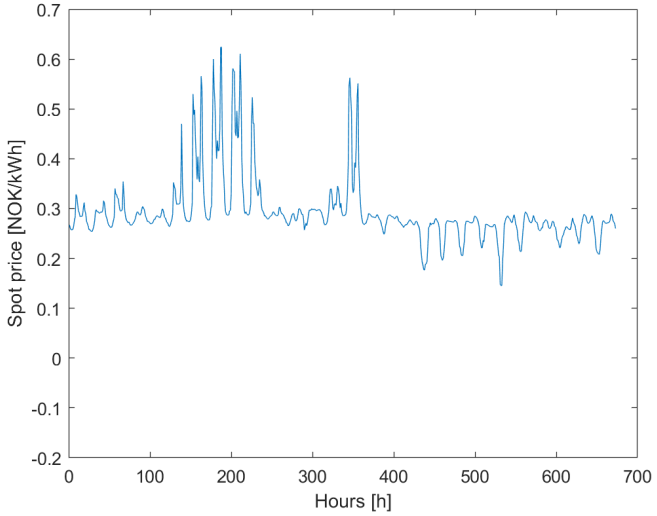

(a) Sweden (SE1)

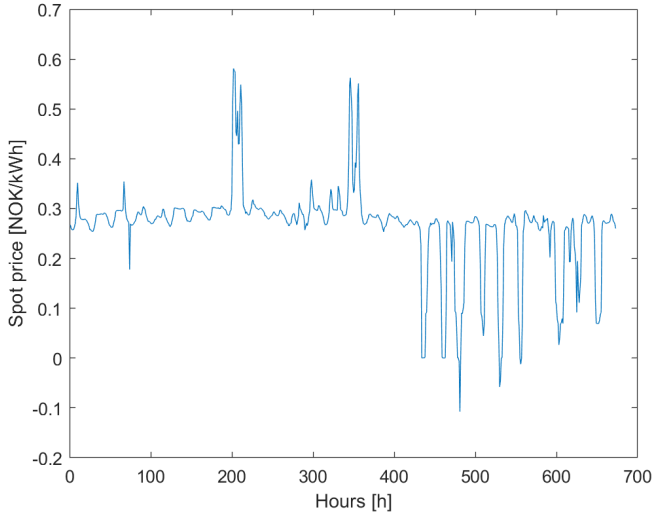

(b) Denmark (DK1)

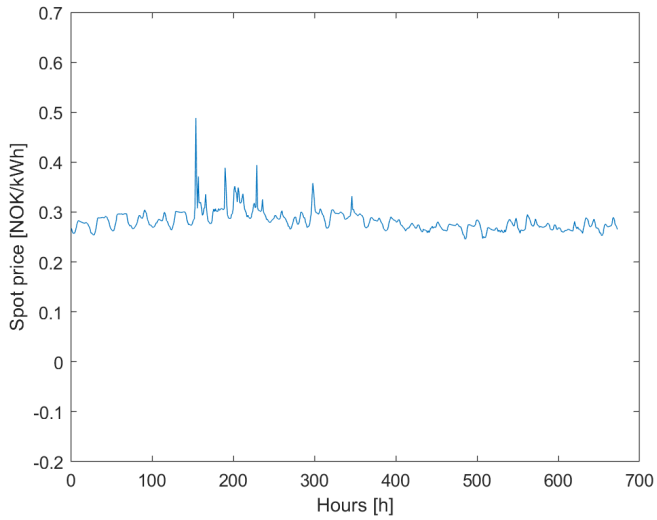

(c) Norway (Oslo)

Figure 6.7: Elspot day-ahead prices for different areas (2017), based on data from [6]

The last figure shows the day-ahead prices for Oslo, i.e. the spot prices used in all previous case studies in this paper. As can be seen from the figures, the day-ahead prices for Oslo are relatively stable compared to the prices for Sweden (SE1) and Denmark (DK1). Moreover, the prices for Denmark are more volatile with the day-ahead prices being negative for several hours. This phenomenon can occur when the power generation from high inflexible sources, like nuclear power plants or wind plants, exceeds the demand as they cannot be shut down and restarted in a cost-efficient manner [41]. Although the market price is negative, owners of renewable power plants are still guaranteed a revenue due to the Danish policy: all renewable generation receive a bonus on top of the market price [42]. This poses a potential problem, as the owner of a renewable power plant has no incentive to turn off the generation during negative prices, as this may be more expensive than selling power for a negative price.

In the following analysis, the simulations have been carried out on a 150 kWh battery for different Elspot day-ahead prices to see how this would affect the optimal results. Table 6.4 gives an overview of the resulting total system cost, both with and without a BESS.

Table 6.4: Total system cost for an arbitrary month using different spot prices

	Oslo	**Sweden (SE1)**	**Denmark (DK1)**
System without BESS	139,016 NOK	141,262 NOK	135,624 NOK
System with BESS	129,055 NOK	131,180 NOK	125,280 NOK
Net savings	9,961 NOK (7.17%)	10,082 NOK (7.14%)	10,344 NOK (7.63%)

In order to see how the system operates under more volatile prices, the results using the spot prices from Denmark are presented in Fig. 6.8.

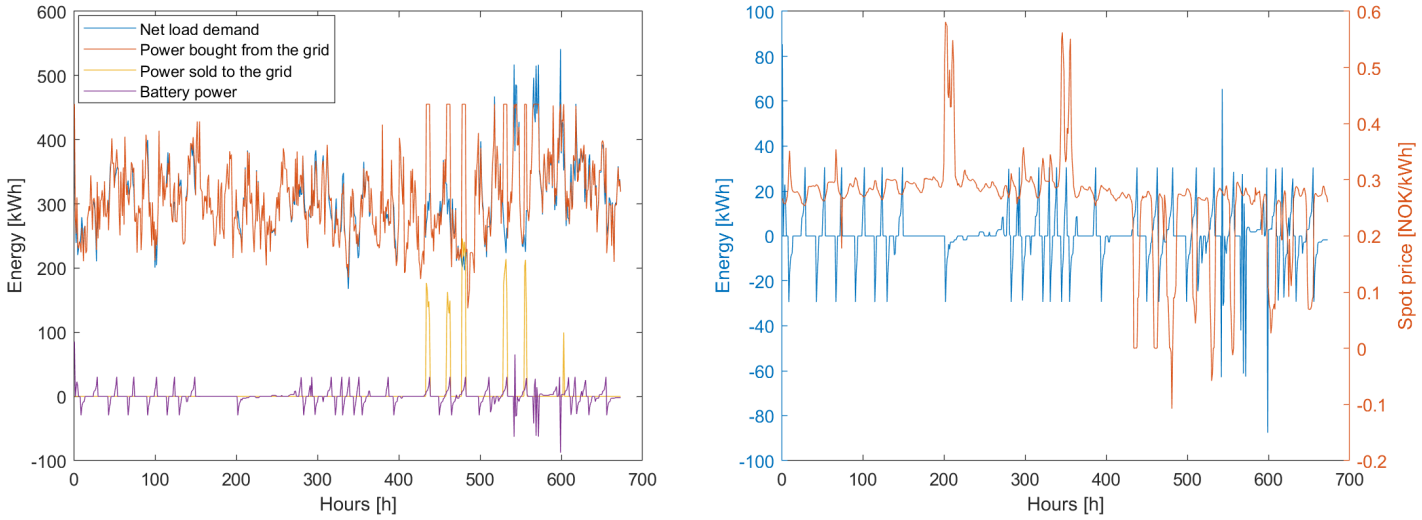

(a) System operation

(b) Battery operation and spot prices

Figure 6.8: System operation using the DK1 spot prices

As seen from Fig. 6.8a, the power sold to the grid is no longer zero as for the BC. This has a correlation with the spot prices, as seen when comparing Fig. 6.8a and 6.8b: when the spot prices are zero or negative, it is economically attractive to buy as much power as possible from the grid without exceeding the limits, and feed the excess power back to the grid. However, this is not possible in real life: in order for power to be fed back to the grid, it has to come from either excess solar production or from discharging the battery. Moreover, it can be seen from Fig. 6.8b how the battery charges when the spot prices are low and discharges when they are higher, thus performing price arbitrage operation.

The battery operation under both Norwegian and Danish spot prices are shown in Fig. 6.9. As seen, the battery is slightly more active when subject to Danish spot prices due to the prices being more volatile.

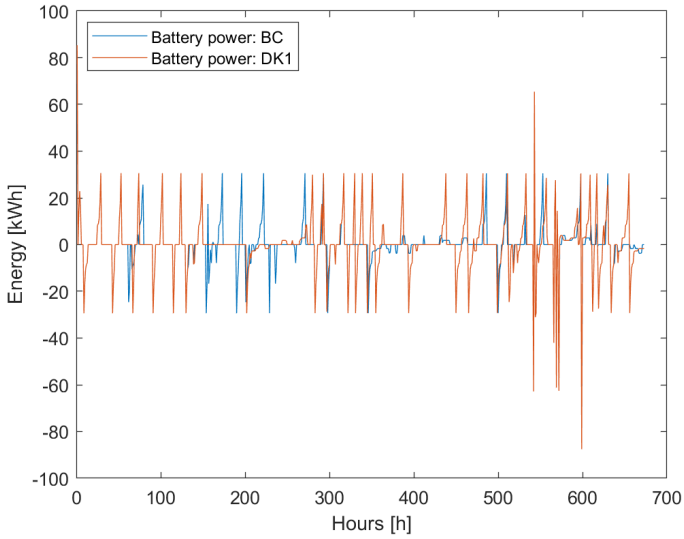

Figure 6.9: Battery operation: Norwegian and Danish spot prices

6.4 System Operation in the Future: a 2030 Scenario

While the sensitivity analyses presented above give an indication on the operational trends when changing important parameter values, they are only simulated for an arbitrary month in order to save simulation time. Moreover, the different analyses study the impact of changing one parameter while keeping the others constant. In the following analysis, the system is simulated for one year using parameter values corresponding to future trends. More specifically, the following assumptions are made on the parameter values for the year 2030:

- The cost of the battery storage system, c_{bat} is decreased by 50%. As discussed in Section 2.1.2, the cost of a lithium-ion BESS using a NMC battery is expected to decrease by around 55% by 2030.
- The peak demand tariff is increased by 30%.
- The energy tariff is subject to a RTP scheme, as for the BC, using day-ahead prices from Denmark (D1). These prices are chosen to reflect that the Norwegian market is expected to see more volatile prices with higher price peaks in the future due to the vast implementation of inflexible power generation like solar and wind, as discussed in Section 2.3.

6.4.1 The Present Alternative

Table 6.5 gives an overview of the present alternative, i.e. the system without BESS, for the assumed 2030 scenario. When analyzing the results obtained from simulating the proposed system, these values are used as a basis for interpreting whether installing a BESS is economically beneficial. When compared to the present, the cost of energy peak power increase by 2.2% and 30% under a 2030 scenario, respectively. The total system cost is increased by 11.7%.

Table 6.5: The present alternative: 2030 scenario

Grid only	
Energy drawn from the grid (net load)	2,243,653 kWh
Total cost of energy	626,480 NOK
Total cost of peak power	410,737 NOK
Total cost of electricity	1,037,217 NOK

6.4.2 The Proposed System

The yearly operation of the proposed system is optimized for the assumed 2030 scenario, with all other parameters being similar to the ones used in the BC. The simulations were carried out for a battery capacity of both 150 kWh (the optimal value found for the BC) and 490 kWh (the optimal value found for a 50% reduction in c_{bat} for an arbitrary month), showing that a 150 kWh battery resulted in the lowest total system cost. As such, the following results are obtained with a 150 kWh battery.

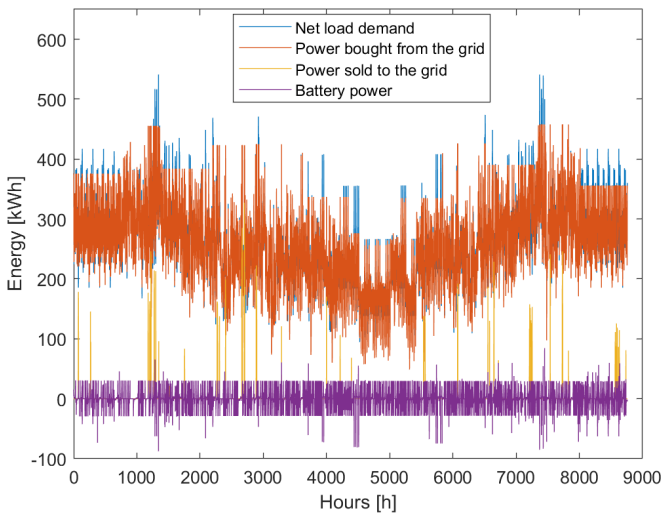

(a) System operation

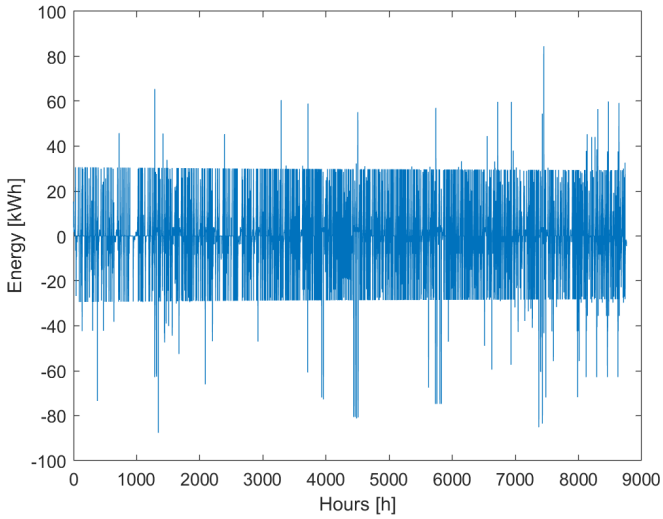

(b) Battery operation

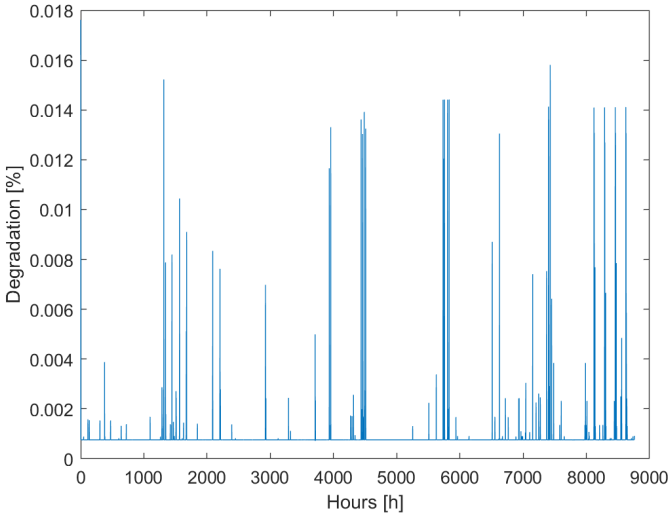

(c) Battery degradation

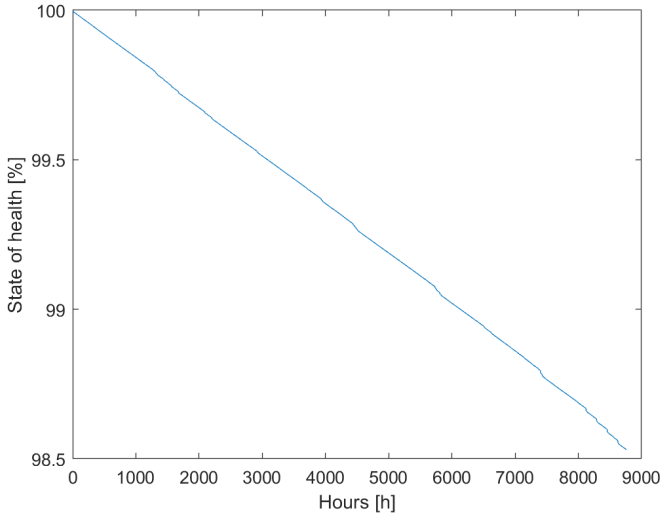

(d) Battery state of health

Figure 6.10: Results for one year: a 2030 scenario

Unlike for the BC (see Fig. 6.1), some power is sold to the grid as seen in Fig. 6.10a. In fact, the total amount of power fed back to the grid during one year is equal to 25,574 kWh. As shown for SA3 in Section 6.3.3, this is due to the spot prices being zero or negative in some hours of the year. It can also be seen that when compared to the BC, the battery is more active due to more volatile prices. However, the SOH at the end of the year for the two scenarios are the same, which is surprising. This can be explained by noting that the battery operation is mostly within the same limits as for the BC, i.e. the battery charges or discharges only small amounts whenever possible to keep the degradation equal to the calendric degradation.

As for the BC, the battery is discharged during high peak demand periods, thus shaving the peaks. An interesting find is that although increasing the peak demand tariff, the amount of peak shaved is equal to that of the BC for all months. This is due to the size of the battery being equal for the two cases, and the peak power demand being limited by the usable capacity of the battery.

A summary of the most important results are listed in Table 6.6, and analyzed below.

Table 6.6: Results from simulating the proposed system using a 2030 scenario

Results: a 2030 scenario	
Energy drawn from the grid	2,272,023 kWh
Compared to original system (2030)	*+ 28,370 kWh*
Compared to the BC	*+ 26,739 kWh*
Feed-back to the grid	25,574 kWh
Revenue generated from feed-back	1,023 NOK
Total degradation	1.47%
Total cost of degradation	19,836 NOK
Compared to original system (2030)	*+ 19,836 NOK*
Compared to the BC	*- 18,800 NOK*
Total cost of energy	622,383 kWh
Compared to original system (2030)	*- 4,097 NOK*
Compared to the BC	*+ 10,271 kWh*
Total cost of peak power	353,041 NOK
Compared to original system (2030)	*- 57,696 NOK*
Compared to the BC	*+ 81,043 kWh*
Total system cost (objective function)	994,238 NOK
Compared to original system (2030)	*- 42,979 NOK*
Compared to the BC	*+ 71,491 kWh*

When comparing the obtained results with the original system under a 2030 scenario, the following observations can be made:

- There is a much higher amount of energy drawn from the grid than for the original system. This is due to the battery being charged by the grid, but also because there is a large amount of power fed back to the grid.
- Although the amount of energy drawn from the grid is higher, the cost of energy is lowered by 0.7% when implementing a BESS due to the battery being used for price arbitrage operation. This is an increase of 0.6% from the BC results. As such, price arbitrage operation is increasingly beneficial with more volatile spot prices, as can be expected.
- The cost of peak power is reduced by implementing a BESS, more specifically by 14.1% - an increase of 0.2% from the BC results.
- The total system cost is reduced by 4.15% by implementing a BESS. This is a substantial improvement from the BC, where the system cost is reduced by 0.64%.

When compared to the BC however, it can be seen that:

- The cost of energy is increased by 1.68%. This is likely due to the spot prices for Denmark being higher on average than the Norwegian prices. However, the percentage increase is lower than for the original system (2.2%).
- The cost of peak power is increased by 29.8% due to the increase in the peak demand tariff. However, the percentage increase is lower than for the original system (30%).
- The total cost of degradation is almost halved due to the reduction in the cost of the battery.
- The total system cost increases by 7.8%. For comparison, the system cost for the original system increases by 11.7%.

In order to be able to study the system operation in more detail, the results for an arbitrary week 8 are shown in Fig. 6.11.

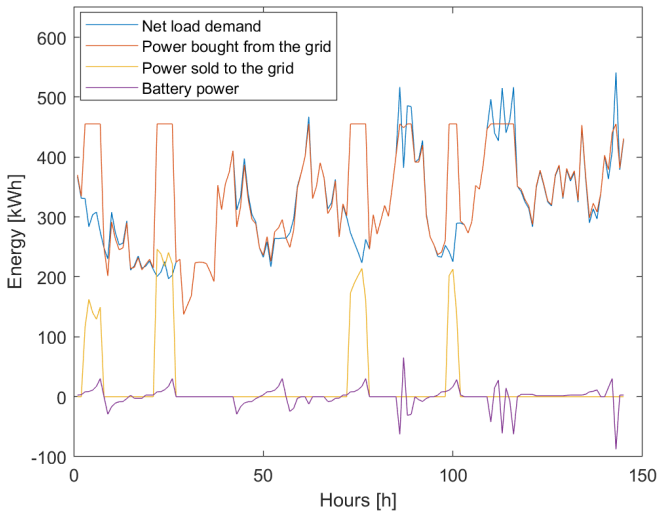

(a) System operation

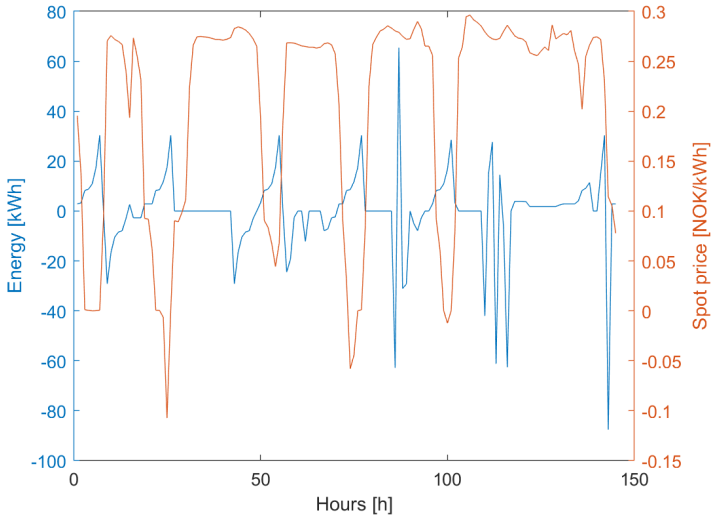

(b) Battery operation and spot prices

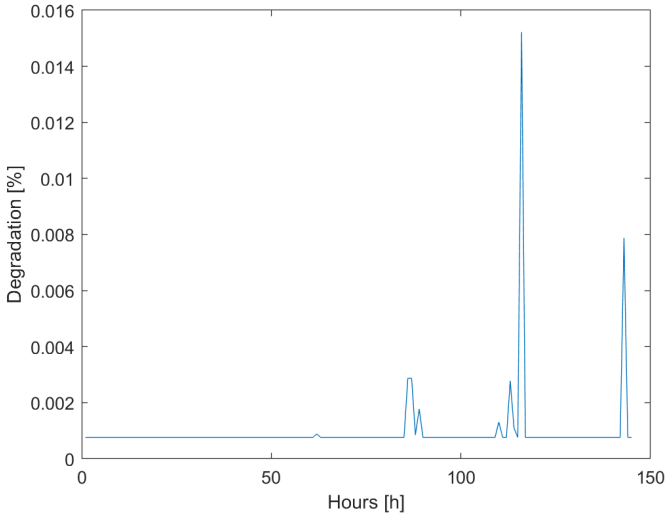

(c) Battery degradation

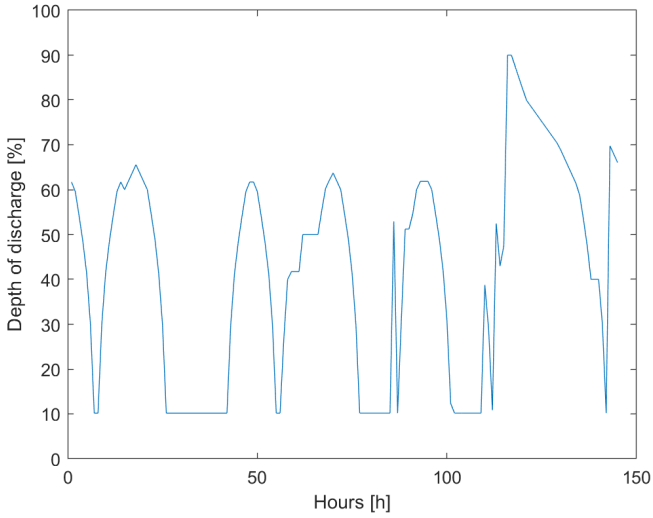

(d) Battery depth of discharge

Figure 6.11: Results for week 8: a 2030 scenario

By studying the figures above, several observations can be made:

- As shown for SA3 in Section 6.3.3, when subject to spot prices equal to or below zero the system chooses to buy as much power as possible from the grid within limitations, and feed the excess power back to the grid after supplying the load and charging the battery. Doing so generates a revenue for the customer, however it is not a valid result due to physical limitations as discussed in Section 6.3.3.

- As for the BC, the battery chooses to charge during hours of low spot prices, and discharge

when the prices are high, resulting in net savings on the energy bill. During hours of high peaks the battery operates regardless of the spot price: for around hour 90, it can be seen how the battery needs to be charged during a relatively high spot price (0.27 NOK) in order to shave the peak in the next hour.

- As for the BC, the battery degradation is high during hours of high peaks.
- When looking at Fig. 6.11b and Fig. 6.11c and comparing them with the BC, it becomes evident that the battery operations are approximately similar. This is due to the load profile being equal for both cases, and the battery prioritizing shaving peaks due to the high peak demand tariffs. However, the battery under a 2030 scenario is more active due to the Danish spot prices being more volatile. This is also seen when comparing the DOD-curve for the two cases.

7 | Discussion

The purpose of this study is to see whether implementing a battery storage system into an existing grid-connected photovoltaic (PV) system could provide benefits for the customer in terms of cost savings, while optimally operating the battery such as to minimize its degradation. Recall that the customer in this case is an energy efficient swimming facility located in Norway. In this chapter, the main findings from the results presented in Chapter 6 are discussed, as well as the validity of the simulation model and the assumptions made.

7.1 The Base Case (BC)

The simulation results from the BC reveal that installing a battery energy storage system (BESS) is economically attractive for the customer already today, with a net savings on the total system cost of 0.64% yearly. This includes the cost of the battery, which is accounted for in the degradation cost. Interestingly, this finding collides with other research. Hesse et. al [12] found that including a BESS gave almost consistently negative rate of investments for nickel manganese cobalt oxide (NMC) batteries, except for very small load demands, when using flat-rate energy tariffs from Germany. Dufo-Lõpez [10] found that even when considering a reduction in the cost of battery storage and an hourly real-time pricing (RTP) scheme, the optimal battery size was not profitable for the system under study. However, these articles are concerned about residential customers and do not consider the impact of the peak demand charge, hence the battery is not used for peak shaving purposes. The simulation results from the BC show that using the battery for peak shaving purposes is highly beneficial, which was also found in a different case study by Shi et. al [43]. For the BC, the cost of peak demand is reduced by 13.9%, making peak shaving operation by far the largest contributor to the net cost savings. In fact, the savings from peak shaving alone exceeds the cost of battery degradation, and is thus enough to compensate for the yearly cost of the battery. However, keep in mind that the yearly cost of the battery is a percentage of the initial investment cost - a

one-time investment which may be substantial. Moreover, net present cost calculations are omitted in this study, and would have to be included if the simulations are to be done over several years.

The results from the BC also show that the net load demand is always positive, i.e. solar production never exceeds load demand. As such, for the battery to operate it needs to be charged by the grid, which is generally considered unfavorable due to losses in the BESS. In a study by Ranaweera et. al [5], the optimal solution for the case with a positive net load demand was to keep the battery idle, i.e. non-operative, for all hours. The study considered time-of-use (TOU) pricing, however under a RTP scheme the battery offers an advantage: price arbitrage. As shown in the results, the battery charges from the grid during hours of low spot prices, and discharges to supply the load when the spot prices are high. As such, even though the amount of energy drawn from the grid is higher than for the original system, implementing a BESS reduces the cost of energy by 0.1%. By performing price arbitrage operations, the battery is thus able to account for all the energy it draws from the grid and still provide cost savings, implying that implementing a battery could be beneficial even without a PV system. However, Holmen swimming facility is currently billed using a flat rate energy tariff, making price arbitrage operation unachievable. Nevertheless, RTP schemes are expected to become more popular with the introduction of smart meters as discussed in Section 2.3. When the time comes that customers can choose a pricing scheme based on the hourly spot prices, implementing a BESS would be economically attractive for the facility.

An interesting find from the BC is related to the operational pattern of the battery: for most hours, the battery chooses to charge or discharge only small amounts whenever possible. This is related to the degradation model, where the total degradation in each time step is equal to the maximum of either the calendric or the cyclic aging. Seeing as the objective function includes the cost of degradation, which in turn is proportional to the total degradation, the optimization model attempts to minimize the degradation in each time step. However, the minimum value the total degradation can take is the calendric aging, which is modelled as a constant. Moreover, this ensures that the battery can load up on energy which can later be used for discharging during hours of high peaks. However, these results highlight a flaw in the model formulation. Recall that the degradation model used in the simulations, where the total degradation is set to be the maximum of either the calendric or the cyclic aging, is based on the assumption that the cyclic aging will always be higher than the calendric aging when the battery is operating. The results from the BC show that this does not hold.

However, using a more complex degradation model would not necessarily lead to a different result: there would still be a cost of keeping the battery idle, and the results show that it is more beneficial to operate the battery while ensuring minimal cyclic degradation. It should also be noted that the cyclic degradation model is based on the DOD versus cycle life curve of a NMC battery (Fig. 2.2), and the results will therefore vary depending on the battery chemistry.

The results also reveal a correlation between the degradation and the DOD in each time step, due to the cyclic degradation model being based on the DOD versus cycle life curve. More specifically, it is shown how deep discharge operation amounts to a high cost of degradation due to the low expected cycle life of high discharge levels. As such, deep discharge is avoided whenever possible, which is in line with the theory. Nevertheless, during hours of high power peaks, the battery chooses to discharge large amounts of power regardless of the degradation costs. This is due to the cost savings from peak shaving far exceeding the resulting operational costs. An example was shown for February, where the savings from peak shaving in one hour amounted to 12,874 NOK compared to the operational costs of 64.7 NOK.

The total degradation of the battery for a one year operation is found to be 7.15%, meaning it could theoretically operate another 14 years assuming no changes in the system characteristics. With a calendric lifetime of 15 years, i.e. the expected lifetime when keeping the battery idle, using the battery for both peak shaving and price arbitrage operations only reduces the expected lifetime by one year, while providing yearly net savings for the customer. This shows the importance of including the cost of battery degradation in the objective function: without considering this cost, the battery would have been operated in a more aggressive manner. Although perhaps providing higher yearly revenue, the battery lifetime would be decreased, likely resulting in an overall loss as compared to the case where the cost of degradation is included.

7.2 Sensitivity Analyses

7.2.1 SA1 and SA2

The simulation results from SA1 (decreasing the cost of the battery) and SA2 (increasing the peak demand tariff) reveal that an increase in the peak demand tariff has the highest impact on the simulation results: compared to the BC, a 50% increase in c_{peak} increases the total system costs by 25.6%,

while a 50% decrease in c_{bat} decreases the system costs by only 2.6%. Recall that these results are obtained using a one month time horizon, and with the optimal size of the battery for each scenario. These findings imply that the system is more sensitive to changes in the peak demand tariff than changes in the cost of the battery, due to the cost of peak power contributing to a large part of the total system costs. This is further shown when comparing the cost of peak power and the cost of energy for the system with and without BESS: for a 50% increase in c_{peak}, the increase in the peak demand costs are 38.7% and 50% for the system with and without BESS, respectively. The cost of energy is however approximately equal for the two systems. This shows how the cost of peak power will contribute to a larger share of the total cost of electricity with increasing peak demand charges, but also how peak shaving will provide even higher cost savings. As such, even though installing a BESS is beneficial today, it will be even more so with increasing demand charges. The same is true for decreasing battery costs.

The fact that the cost of energy is approximately equal for the system with and without BESS for SA1 and SA2 shows how the power drawn from the grid to charge the battery is compensated for by price arbitrage operation. However, even though price arbitrage provides some benefits, it amounts to only a small percentage of the cost savings as compared to performing peak shaving.

The simulation results also show that the optimal size of the battery increases with both increasing c_{peak} and decreasing c_{bat}. This is due to the battery being able to discharge larger amounts of power in each time step, thus reducing the peak power demand and the total system cost. It should be noted that a C-rate of 1 is assumed for the battery, meaning it is able to charge or discharge with the nominal power rating of the inverter in each hour. However, this may not be an acceptable assumption for all battery technologies and sizes. Nevertheless, increasing the battery capacity does not provide substantial cost savings: for a 50% decrease in c_{bat}, increasing the battery capacity from 150 kWh to 500 kWh amounts to only a 0.14% decrease in the system cost. The same trend is true for an increase in the peak demand tariff. As such, a battery capacity of 150 kWh may be preferable regardless of the parameter values due to it being lighter, smaller and having less initial investment costs. It should also be noted that the sensitivity analyses have been carried out for battery capacities up to 500 kWh to save simulation time as the parameters had to be changed manually, which may result is some errors regarding the optimal battery size.

7.2.2 SA3

The simulation results from SA3 (more volatile spot prices) reveal some interesting findings. For one, the Elspot day-ahead market for Denmark (D1) has several hours where the spot prices are zero or negative. Customers under a RTP scheme will thus earn money from drawing more power from the grid when the spot prices are negative, as this will help balance the grid. This is confirmed by the results: during hours of negative spot prices, the power drawn from the grid is as high as possible without exceeding the set limit. This power is used to supply the load and to charge the battery while generating a revenue for the facility. However, the battery is not charged to full capacity as could be expected when the price of electricity is negative: it is only charged up to the limit where the cost of cycling the battery is equal to the cost of calendric aging. Charging the battery with more power would lead to a higher degradation cost, exceeding the possible revenue from charging during hours of negative pricing. Finding the spot price for when it would be economically attractive to fully charge the battery is difficult, as this depends on both the energy in the battery and the DOD at the given hour. However, if assuming a fresh battery and an initial DOD of 90% (the maximum DOD for the simulation model), the resulting spot price would have to be -0.90 NOK/kWh (calculations are shown in Appendix C). Seeing as some of the most negative spot prices for Germany in 2017 were around -0.8 NOK/kWh, and due to the high availability of flexible resources in Norway, like hydro power, this may not be a likely scenario.

The results also show that the remaining power after supplying the load and charging the battery is sold back to the grid directly. With a single metering system and the same contract for buying and selling power, this is not physically possible. However, with two meters and two separate contracts - one for the power bought for the grid, and another for the power sold to the grid - an interesting phenomenon can occur. By drawing large amounts of power from the grid during hours of negative spot prices, and selling the remaining power back to the grid for a feed-in remuneration, the end user can effectively achieve a net income for zero exchange. This highlights a potential problem for the grid in the future, as negative spot prices are an indication of inflexible production exceeding demand, and should encourage users to draw power from the grid for balancing purposes. If the power is sold back to the grid directly, the purpose of balancing is gone. However, as of today there is only one meter. In order to simulate a more realistic scenario, a constraint saying that the power fed to the grid must come from either excess solar production or from discharging the battery could thus be implemented in the model.

As shown for the BC, it is not beneficial to charge the battery and later use that power for feed-in purposes. This is also true for SA3, showing how the battery is never discharged simultaneously as power is fed back to the grid - in fact, it is charged due to the negative spot prices. This is due to the cost of degradation and losses in the battery being higher than the potential revenue from discharging the battery for feed-in remuneration. Moreover, a revenue is gained when charging the battery during negative spot prices. If using the battery for feed-in purposes is to become beneficial for the customer, the feed-in tariff needs to increase. However, this is not a likely scenario: as the installations of small-scale renewables continue to grow, the feed-in tariffs are expected to decrease even further.

7.3 A 2030 Scenario

The results from simulating the assumed 2030 scenario, using a one year time horizon and parameter values as described in Section 6.4, reveal that installing a BESS is even more profitable in the future: the total system cost is decreased by 4.15%, which is a substantial improvement from the 0.64% decrease for the BC. While the percentage reduction in the cost of energy and peak power is not that different from the BC results, the total cost of degradation is almost halved due to the decrease in the cost of the battery. As such, even if the energy and peak demand tariffs remain constant up to 2030, the expected reduction in battery costs will make installing a BESS economically attractive.

The results also show that power is fed back to the grid when the spot prices are negative. As discussed for SA3, this can pose a potential problem for the grid in the future if separate metering systems and contracts are made available. However, as of today this is not yet possible. Nevertheless, the revenue from selling power back to the grid only amounts to 2.4% of the total cost savings. As such, it is not a crucial part of the system economics.

An interesting find is that although the battery is more active in a 2030 scenario, due to the spot prices being more volatile, the degradation is the same as for the BC. This is due to the battery only charging or discharging small amounts of power whenever possible, as previously discussed, to keep the cyclic aging equal to the constant calendric aging, thus minimizing the cost of degradation. Recall that the same battery size of 150 kWh has been used for both scenarios. Moreover, the peak shaving profile remains unchanged for the 2030 scenario, and as such the degradation during peak hours is

similar to the BC. This shows how increasing the peak demand tariff has no effect on the resulting peak shaving amount - the optimization model will always choose to minimize the peak demand due to the high cost of peak power, and as such the peak shaving amount is only limited by the battery capacity. Moreover, these results show how the battery will prioritize peak shaving operations regardless of the spot price due to the savings from performing peak shaving exceeding the cost of operation.

7.4 Assumptions

When viewing and analyzing the results, it should be kept in mind that several simplifications and assumptions have been made in order to model the system. In this section, key assumptions that have not been discussed in the previous sections are explored. Firstly, the load demand and solar production are estimated based on historical data. Seeing as the actual load and production profiles for Holmen swimming facility will deviate from these estimations, perhaps by a lot, the simulation results will differ from the BC. However, the operational trends will stay the same: the battery will choose to operate in a way that minimizes the cost of degradation while both performing price arbitrage and peak shaving, hence the resulting cost of energy and peak power are likely to be reduced. Nevertheless, the operational trends can differ if the solar production exceeds the load demand in any hour. If so, the excess production can either be used to charge the battery or for feed-in remuneration. However, this is not a likely scenario as the PV system is much too small to ever exceed the load demand as of today.

Secondly, due to the simulation being carried out using estimations on the hourly load demand and solar production, as well as the energy tariffs, a perfect forecast model is assumed. As such, the results obtained for hourly operation are optimized using known values. In reality, the load demand and solar production are not known prior to solving, and are affected by a range of external factors: outside temperature, the number of visitors to the swimming facility, solar irradiation, if there are clouds in the sky or not, and so on. As such, if the battery is to be optimally controlled hour by hour, a forecasting algorithm taking these factors into account should be implemented in the model. However, this is outside the scope of this thesis and is thus not discussed further.

8 | Conclusion

In this thesis, the economic benefits of implementing battery storage into an existing grid-connected PV system is studied. The objective is to minimize the total system cost, including the cost of energy, the cost of peak power and the operational cost of the battery. The main purpose of the battery is to shave the peak power demand, as this contributes to a large part of the monthly energy bill. An optimization model based on multi integer linear programming is built, and simulated using a one year time horizon in GAMS and Matlab. Several studies are carried out using Holmen swimming facility as test case, however the model can easily be adapted to fit any load and solar profile. In this chapter, the most important conclusions drawn from the results and discussions are presented.

The results reveal that installing a battery storage system is economically attractive for the customer already today, with a net savings on the total system cost of 0.64% yearly. The cost of peak power demand is reduced by 13.9%, and the savings from peak shaving operation alone is enough to compensate for the yearly cost of the battery. The results also show that even though the battery is charged by the grid, the cost of energy is reduced by 0.1%. As such, the battery is able to account for all energy bought from the grid while still providing cost savings through price arbitrage operations. It should be kept in mind that these results are only valid for a real-time pricing scheme based on hourly spot prices: for constant energy rates, price arbitrage operation is unattainable. It is also found that, due to the low feed-in tariffs of today, it is never beneficial to discharge the battery for feed-in remuneration.

An interesting finding is that the battery chooses to operate in a matter that keeps the cyclic aging equal to the calendric aging, thus charging or discharging only small amounts of power each time step. In this way, the battery can perform price arbitrage operations while keeping the cost of degradation to a minimum. Even during hours of negative spot prices the battery only charges up to this limit, as the cost of degradation exceeds the possible revenue from charging with negative prices.

The resulting degradation is found to be 7.15% yearly, meaning the battery could operate another 14 years assuming no changes in the system characteristics.

The results from the sensitivity analyses show that the system is more sensitive to changes in the peak demand tariff than changes in the cost of the battery: compared to the BC, a 50% increase in c_{peak} increases the total system costs by 25.6%, while a 50% decrease in c_{bat} decreases the costs by only 2.6%. Moreover, it is found that increasing the size of the battery over 150 kWh does not provide substantial cost savings, regardless of the parameter values. As such, a battery capacity of 150 kWh is recommended for the system as it is both lighter, smaller and has less initial investment costs. It is also shown that for negative spot prices, maximum power is drawn from the grid, and the remaining power after supplying the load and charging the battery is sold back for a feed-in remuneration. This can be made possible with two separate metering systems and contracts, and may pose a potential problem for the grid in the future as the end user can effectively achieve a net income for zero exchange.

The simulations are also carried out using an assumed 2030 scenario, where the cost of the battery is reduced, the peak demand charge is increased and the spot prices are more volatile. The results reveal that implementing a battery storage system is even more profitable in the future: the total system costs decrease by 4.15%. Moreover, due to the spot prices being more volatile, the battery performs more price arbitrage operation and is thus more active than for the BC. Interestingly, the total degradation for the two scenarios is the same. This is due to the battery keeping its operation within the limits of the calendric degradation when performing price arbitrage as previously mentioned. Moreover, due to the battery capacities being equal, the resulting amount of peak shaved is similar. As such, it can be concluded that the peak shaving is only limited by the battery capacity, as the optimal solution will always be to shave as much of the peak demand as possible due to the high costs of peak power.

8.1 Shortcomings and Further Work

Below, the main shortcomings of the study and suggestions for further work are listed.

- As proven by the results, the assumption that the cyclic aging is always higher than the calendric aging when the battery is operating does not hold. A more realistic modelling of

the total degradation could improve the simulation results, however this would also make the model more complex.

- As mentioned, the results show that during negative spot prices, power is bought from the grid and directly fed back to the grid for a feed-in remuneration. Although posing a potential problem for the grid in the future, this is not yet made possible due to the single metering system. As such, the model could be made more realistic by imposing a constraint on the power sold to the grid: it can only come from excess solar production, or from discharging the battery.

- A perfect forecasting algorithm is assumed in this thesis, meaning the load demand, solar production and spot prices are known prior to solving the optimization problem. In reality, this is not possible, however the model needs a way to estimate these parameters in order to optimally control the battery. A further improvement of the model could thus be implementing a forecasting algorithm.

- The yearly load demand and solar production used in the simulation model are based on estimates, as historical data was only available for the first part of 2018. As such, to validate the profitability of implementing battery storage, the model should be run when data is available for a whole year.

Bibliography

[1] Y. Wang, Z. Zhou, A. Botterud, K. Zhang, and Q. Ding, "Stochastic coordinated operation of wind and battery energy storage system considering battery degradation," *Journal of Modern Power Systems and Clean Energy*, vol. 4, 2016. [Online]. Available: https://link.springer.com/content/pdf/10.1007{%}2Fs40565-016-0238-z.pdf

[2] N. Omar, M. A. Monem, Y. Firouz, J. Salminen, J. Smekens, O. Hegazy, H. Gaulous, G. Mulder, P. Van den Bossche, T. Coosemans, and J. Van Mierlo, "Lithium iron phosphate based battery – Assessment of the aging parameters and development of cycle life model," *Applied Energy*, vol. 113, pp. 1575–1585, jan 2014. [Online]. Available: https://www.sciencedirect.com/science/article/pii/S0306261913007393{#}s0020

[3] Y. Yang, H. Li, A. Aichhorn, J. Zheng, and M. Greenleaf, "Sizing Strategy of Distributed Battery Storage System With High Penetration of Photovoltaic for Voltage Regulation and Peak Load Shaving," *IEEE Transactions on Smart Grid*, vol. 5, no. 2, pp. 982–991, mar 2014. [Online]. Available: http://ieeexplore.ieee.org/document/6609116/

[4] International Renewable Energy Agency (IRENA), *Electricity storage and renewables: Costs and markets to 2030*, 2017, no. October. [Online]. Available: http://irena.org/publications/2017/Oct/Electricity-storage-and-renewables-costs-and-markets

[5] I. Ranaweera and O. M. Midtgård, "Optimization of operational cost for a grid-supporting PV system with battery storage," *Renewable Energy*, vol. 88, pp. 262–272, 2016. [Online]. Available: http://dx.doi.org/10.1016/j.renene.2015.11.044

[6] Nord Pool, "Historical Market Data." [Online]. Available: https://www.nordpoolgroup.com/historical-market-data/

[7] Hafslund Net, "Priser på nettleie - bedrift." [Online]. Available: https://www.hafslundnett.no/artikler/nett-og-nettleie/priser-bedrift/1hqF2AQY1Ay8uW0a6i0S20

[8] Statnett, "Fleksibilitet i det nordiske kraftmarkedet," 2018. [Online]. Available: https://www.statnett.no/Global/Dokumenter/Media/Nyheter2018/Fleksibilitetidetnordiskekraftmarkedet2018-2040.pdf

[9] H. Dagdougui, N. Mary, A. Beraud-Sudreau, and L. Dessaint, "Power management strategy for sizing battery system for peak load limiting in a university campus," in *2016 IEEE Smart Energy Grid Engineering (SEGE)*. IEEE, aug 2016, pp. 308–312. [Online]. Available: http://ieeexplore.ieee.org/document/7589542/

[10] R. Dufo-López, "Optimisation of size and control of grid-connected storage under real time electricity pricing conditions," *Applied Energy*, vol. 140, pp. 395–408, feb 2015. [Online]. Available: https://www.sciencedirect.com/science/article/pii/S0306261914012616

[11] A. Nottrott, J. Kleissl, and B. Washom, "Energy dispatch schedule optimization and cost benefit analysis for grid-connected, photovoltaic-battery storage systems," *Renewable Energy*, vol. 55, pp. 230–240, jul 2013. [Online]. Available: https://www.sciencedirect.com/science/article/pii/S0960148112008026

[12] H. C. Hesse, R. Martins, P. Musilek, M. Naumann, C. N. Truong, and A. Jossen, "Economic optimization of component sizing for residential battery storage systems," *Energies*, vol. 10, no. 7, 2017.

[13] K. Abdulla, J. de Hoog, V. Muenzel, F. Suits, K. Steer, A. Wirth, and S. Halgamuge, "Optimal Operation of Energy Storage Systems Considering Forecasts and Battery Degradation," *IEEE Transactions on Smart Grid*, pp. 1–1, 2016. [Online]. Available: http://ieeexplore.ieee.org/document/7562406/

[14] J. Weniger, T. Tjaden, and V. Quaschning, "ScienceDirect Sizing of residential PV battery systems," *Energy Procedia*, vol. 46, pp. 78–87, 2014. [Online]. Available: www.sciencedirect.com

[15] C. Truong, M. Naumann, R. Karl, M. Müller, A. Jossen, and H. Hesse, "Economics of Residential Photovoltaic Battery Systems in Germany: The Case of Tesla's Powerwall," *Batteries*, vol. 2, no. 2, p. 14, may 2016. [Online]. Available: http://www.mdpi.com/2313-0105/2/2/14

[16] A. Joseph and M. Shahidehpour, "Battery storage systems in electric power systems," *IEEE Power Engineering Society General Meeting*, pp. 8 pp.–, 2006.

[17] IRENA, "Battery Storage for Renewables: Market Status and Technology Outlook," 2015. [Online]. Available: http://www.irena.org/-/media/Files/IRENA/Agency/Publication/2015/IRENA{_}Battery{_}Storage{_}report{_}2015.pdf

[18] A. Eller and D. Gauntlett, "Energy Storage Trends and Opportunities in Emerging Markets," 2017. [Online]. Available: https://www.ifc.org/wps/wcm/connect/ed6f9f7f-f197-4915-8ab6-56b92d50865d/7151-IFC-EnergyStorage-report.pdf?MOD=AJPERES

[19] J. Vetter, P. Novák, M. R. Wagner, C. Veit, K.-C. Möller, J. O. Besenhard, M. Winter, M. Wohlfahrt-Mehrens, C. Vogler, and A. Hammouche, "Ageing mechanisms in lithium-ion batteries," *Journal of Power Sources*, vol. 147, pp. 269–281, 2005. [Online]. Available: https://las493energy.files.wordpress.com/2014/11/2005{_}vetter{_}jpowsourc.pdf

[20] K. Smith and T. Markel, "PHEV Battery Trade-Off Study," no. January, 2015.

[21] D. Andre, C. Appel, T. Soczka-Guth, and D. U. Sauer, "Advanced mathematical methods of SOC and SOH estimation for lithium-ion batteries," *Journal of Power Sources*, vol. 224, pp. 20–27, feb 2013. [Online]. Available: https://www.sciencedirect.com/science/article/pii/S0378775312015303?via{%}3Dihub

[22] M. A. Ortega-Vazquez, "Optimal scheduling of electric vehicle charging and vehicle-to-grid services at household level including battery degradation and price uncertainty," *IET Generation, Transmission & Distribution*, vol. 8, no. 6, pp. 1007–1016, jun 2014. [Online]. Available: http://digital-library.theiet.org/content/journals/10.1049/iet-gtd.2013.0624

[23] P. Keil, S. F. Schuster, J. Wilhelm, J. Travi, A. Hauser, R. C. Karl, and A. Jossen, "Calendar Aging of Lithium-Ion Batteries," *Journal of The Electrochemical Society*, vol. 163, no. 9, pp. A1872–A1880, jul 2016. [Online]. Available: http://jes.ecsdl.org/lookup/doi/10.1149/2.0411609jes

[24] G. He, Q. Chen, C. Kang, P. Pinson, and Q. Xia, "Optimal Bidding Strategy of Battery Storage in Power Markets Considering Performance-Based Regulation and Battery Cycle Life," *IEEE Transactions on Smart Grid*, vol. 7, no. 5, pp. 2359–2367, sep 2016. [Online]. Available: http://ieeexplore.ieee.org/document/7106509/

[25] J. Schmalstieg, S. Käbitz, M. Ecker, and D. U. Sauer, "A holistic aging model for Li(NiMnCo)O2 based 18650 lithium-ion batteries," *Journal of Power Sources*, vol. 257, pp. 325–334, jul 2014. [Online]. Available: https://www.sciencedirect.com/science/article/pii/S0378775314001876

[26] C. Curry, "Lithium-ion Battery Costs and Market," 2017. [Online]. Available: https://data.bloomberglp.com/bnef/sites/14/2017/07/BNEF-Lithium-ion-battery-costs-and-market.pdf

[27] F. Berglund, "Technical-economical evaluation of a grid-connected PV system with battery storage : A Norwegian case study for a medium-scale sports facility," *Unpublished work*, no. Specialization project, NTNU, 2017.

[28] A.-R. Haitham, M. Malinowski, and K. Al-Haddad, *Power Electronics for Renewable Energy Systems, Transportation and Industrial Applications*. John Wiley & Sons, 2014.

[29] NVE, "Plusskunder - NVE." [Online]. Available: https://www.nve.no/reguleringsmyndigheten-for-energi-rme-marked-og-monopol/nettjenester/nettleie/tariffer-for-produksjon/plusskunder/

[30] ——, "Nettleie - NVE." [Online]. Available: https://www.nve.no/stromkunde/nettleie/

[31] Nord Pool, "Nord Pool Group." [Online]. Available: https://www.nordpoolgroup.com/

[32] Battery University, "Types of Lithium-ion Batteries." [Online]. Available: http://batteryuniversity.com/learn/article/types{_}of{_}lithium{_}ion

[33] "Applications of optimization with Xpress-MP." [Online]. Available: www.dashoptimization.com

[34] A. municipality, "FutureBuilt-prosjekt: Holmen svømmehall." [Online]. Available: https://www.asker.kommune.no/samfunnsutvikling/futurebuilt/holmen-svommehall/

[35] "E-mail correspondence with Solel in May 2018."

[36] Agder Energi, "Plusskunde." [Online]. Available: https://www.aenett.no/bygge-og-grave/produksjon-av-strom/plusskunde/

[37] GAMS, "GAMS - Introduction." [Online]. Available: https://www.gams.com/products/introduction/

[38] R. E. Rosenthal, "A GAMS Tutorial." [Online]. Available: https://www.gams.com/latest/docs/UG{_}Tutorial.html

[39] "E-mail correspondance with SIAT in May 2018."

[40] NRLE, "PVWatts Calculator." [Online]. Available: https://pvwatts.nrel.gov/pvwatts.php

[41] EPEX SPOT, "Negative Prices." [Online]. Available: https://www.epexspot.com/en/company-info/basics{_}of{_}the{_}power{_}market/negative{_}prices

[42] RES LEGAL Europe, "Premium tariff (Law on the Promotion of Renewable Energy)," 2017. [Online]. Available: http://www.res-legal.eu/search-by-country/denmark/single/s/res-e/t/promotion/aid/premium-tariff-law-on-the-promotion-of-renewable-energy/lastp/96/

[43] Y. Shi, B. Xu, D. Wang, and B. Zhang, "Using Battery Storage for Peak Shaving and Frequency Regulation: Joint Optimization for Superlinear Gains," 2017. [Online]. Available: https://arxiv.org/pdf/1702.08065.pdf

Appendices

A Calculating the Operational Cost of the Battery

The revenue from peak shaving operation is given as:

$$S_{shaving,t} = c_{peak,t} \cdot (P^{org}_{peak,t} - P^{new}_{peak,t}) \tag{1}$$

where $c_{peak,t}$ is the peak demand charge, $P^{org}_{peak,t}$ the original peak demand without BESS, and $P^{new}_{peak,t}$ the peak demand with BESS.

The operational cost of the battery can be modelled as:

$$C_{operation,t} = \gamma_t + c_{el,avg} \cdot (P^{org}_{peak,t} - P^{new}_{peak,t}) \cdot \eta^2_{inv} \cdot \eta_{rt} \tag{2}$$

where $c_{el,avg}$ is the energy tariff. Seeing as the charging of the battery occurs in several time steps, the energy tariff is assumed to be equal to the average price of electricity for the given month. The total power discharged from the battery is the original power bought from the grid (assumed to be the total amount of power shaved) minus losses in the inverter and battery.

The parameter values of the month with the highest amount of peak shaving, February, are listed in Table 1.

Table 1: Associated parameter values for February

Variable	Value
t	1342
$P^{org}_{peak,t}$	541.23
$P^{new}_{peak,t}$	455.40
γ_t	42.54
$c_{peak,t}$	150
$c_{el,avg}$	0.28

B BC Results for Week 24

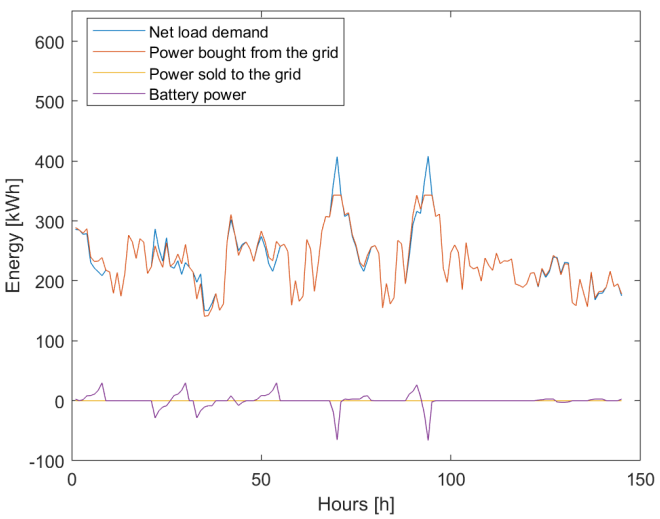

(a) System operation

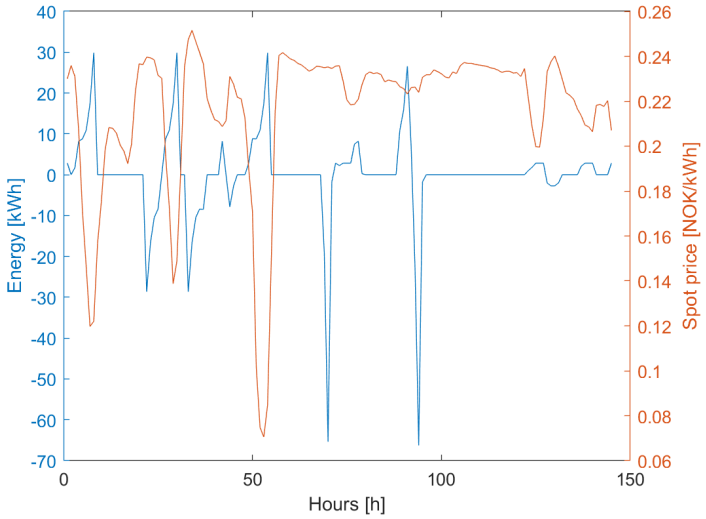

(b) Battery operation and spot prices

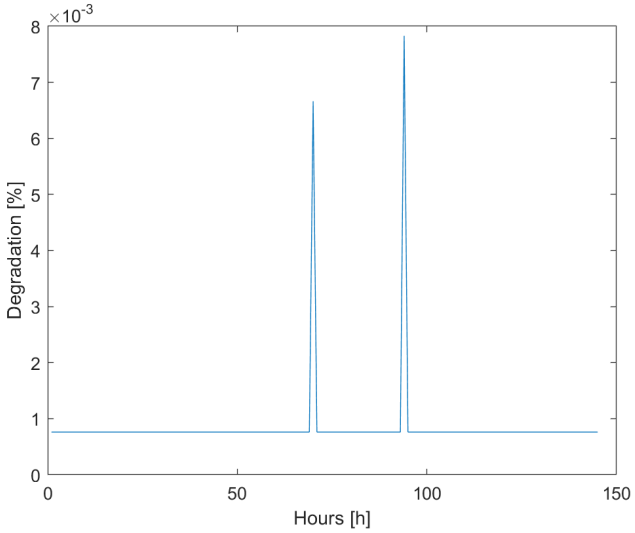

(c) Battery degradation

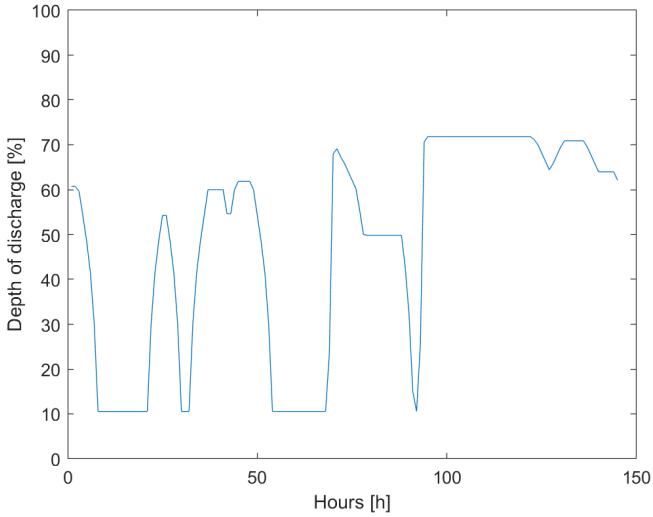

(d) Battery depth of discharge

Figure 1: BC results for week 24

C Calculating the Resulting Spot Price

With a fresh battery and an initial DOD of 90%, the energy content in the battery before time t is:

$$E_{bat,t-1} = E_{bat}^{nom} \cdot SOC_{t-1} = E_{bat}^{nom} \cdot (1 - DOD_{t-1}) = 150\text{kWh} \cdot 0.1 = 15\text{kWh} \tag{3}$$

In order to fully charge the battery, the charging power has to be equal to:

$$P_{charge,t} = \eta_{charge} \cdot (E_{bat}^{nom} \cdot (SOC_{max} - SOC_{min} - E_{bat,t-1}) = 0.98 \cdot (150 \cdot (0.9 - 0.1) - 15)\text{kWh} = 102.9\text{kWh} \tag{4}$$

The power that has to be bought from the grid in order to charge the battery is equal to:

$$P_{grid,b,t} = \frac{P_{charge,t}}{\eta_{inv}} = \frac{102.9}{0.98}\text{kWh} = 105\text{kWh} \tag{5}$$

The degradation cost of fully charging the battery (from 90% DOD to 10% DOD) is:

$$\gamma_t = C_{bat} \cdot DP_t = c_{bat} \cdot E_{bat}^{nom} \cdot 0.5 \cdot |(\rho_t - \rho_{t-1})| = 3,600 \cdot 150 \cdot 0.5 \cdot |\frac{1}{45000} - \frac{1}{2700}| = 94\text{NOK} \tag{6}$$

In order for it to be beneficial to fully charge the battery, the revenue from buying power from the grid at a negative spot price has to be greater than or equal to the cost of charging the battery:

$$c_{el,t} \cdot P_{grid,b,t} \geq \gamma_t \tag{7}$$

As such, the resulting spot price is:

$$c_{el,t} \geq \frac{\gamma_t}{P_{grid,b,t}} = \frac{-94\text{NOK}}{105\text{kWh}} = -0.90\text{NOK/kWh} \tag{8}$$